CReAM
Centre for Research & Analysis of Migration

Discussion Paper Series

CDP 22/20

- **The Role of Schools in Transmission of the SARS-CoV-2 Virus: Quasi-Experimental Evidence from Germany**

- Clara von Bismarck-Osten, Kirill Borusyak, and Uta Schönberg

Centre for Research and Analysis of Migration
Department of Economics, University College London
Drayton House, 30 Gordon Street, London WC1H 0AX

www.cream-migration.org

The Role of Schools in Transmission of the SARS-CoV-2 Virus: Quasi-Experimental Evidence from Germany

Clara von Bismarck-Osten[*], Kirill Borusyak[*†], and Uta Schönberg[*‡]

[*] University College London; [†] CEPR; [‡] IAB, RWI, and CReAM

November 20, 2020

Abstract

This paper considers the role of school closures in the spread of the SARS-CoV-2 virus. To isolate the impact of the closures from other containment measures and identify a causal effect, we exploit variation in the start and end dates of the summer school and fall holiday across the 16 federal states in Germany. Leveraging a difference-in-differences design with staggered adoption, we show that neither the summer closures nor the closures in the fall have had any significant containing effect on the spread of SARS-CoV-2 among children or any spill-over effect on older generations. We also do not find any evidence that the return to school at full capacity after the summer holidays increased infections among children or adults. Instead, we find the number of children infected increased during the last weeks of the summer holiday and decreased in the first weeks after schools reopen, a pattern we attribute to travel returnees and increased testing.

Keywords: Covid Economics, School Closures, Public Health

JEL codes: I10, I18, I28

1 Introduction

The coronavirus pandemic has sparked an international debate on the efficiency of school closures as a containment measure. As a "second wave" of infections by the SARS-CoV-2 virus (causing the "COVID-19" disease) is hitting most European countries, the debate is all the more relevant. The start of the new academic school year and a simultaneous surge in the representation of children among new cases in the fall 2020 (New York Times, 2020; The Guardian, 2020; ZEIT, 2020) are adding to the pressure to understand the role of schools in transmission of the SARS-CoV-2 virus.

Because of their widespread consequences, school closures were among the most controversial containment policies during the first wave of the pandemic. Prolonged school closures may have a negative effect on the psychological and emotional development of children, and unequal remedial measures have been found to widen learning inequalities (Engzell et al., 2020). School closures also negatively impact the careers of parents obliged to take on more educational responsibilities and reduce the number of hours supplied in the labour market, which ultimately lowers GDP (Fuchs-Schündeln et al., 2020). Since women typically shoulder most of the childcare responsibilities, school closures are also feared to widen the gender wage gap in the long run (Alon et al., 2020).

These costs are weighed against the effectiveness of school closures as a strategy to contain the spread of SARS-CoV-2. The main mechanism through which school closures are expected to be effective is by preventing social interactions among children in schools. Reduced contact between children may further break the chain of infection from child to parent and grandparent, thereby reducing infection rates in the adult population. School closures may also induce a series of either offsetting or reinforcing behavioural adjustments. On the one hand, children may substitute school interactions with other activities that introduce additional risks of transmission. On the other hand, school closures could force parents to work from home, reducing their work-related contacts and, thereby, their risk of contagion.[1]

We aim to identify the effect of school closures on children as well as various age groups of adults. Understanding the "spill-over" effects on adults is of central importance, as the severity of the disease has been found to be closely linked to age. Adults are relatively overrepresented among confirmed COVID-19 cases and have a higher risk of dying from the disease, with 95% of the deaths in Germany attributed to the group aged 60 and above. Children under the age of 15, by contrast, account for only 7.2% of Germany's cumulative confirmed SARS-CoV-2 cases, despite making up

[1] A more worrying labour force response would constitute in the reduction of the health-care workforce available. A study in the United States estimates that a total of 28.8% of healthcare providers have childcare obligations (Bayham and Fenichel, 2020).

13.6% of the country's population.[2] They generally experience mild symptoms (Wang et al., 2020), although recent reports suggest an increase in the incidence of children experiencing severe inflammatory symptoms, which could be linked to SARS-CoV-2 (Pouletty et al., 2020).

The evidence on the effectiveness of school closures as a containment measure is mixed. Most epidemiological studies zoom into the level of a single school or other small samples to estimate infection rates, which subsequently feed into models that project the spread of the virus in the general population. Recent studies of this kind conducted in France, Germany and Italy have reached vastly conflicting conclusions on plausible infections rates and contagiousness of children (Fontanet et al., 2020; Berner, 2020; Fateh-Moghadam et al., 2020).[3,4]

In this paper, we take a different approach. We consider school closures and openings as "treatments" and apply modern econometric tools to identify the "causal" effects of school closures and openings on SARS-CoV-2 infections among children, as well as their potential spill-over effects on adults. We exploit variation in the start and end dates of school summer holidays across federal states of Germany for difference-in-differences identification, building on the strategy developed by Adda (2016) in the context of influenza, gastro-enteritis, and chickenpox in France. Germany's sixteen states Germany have staggered summer holidays to avoid overcrowding the national travel infrastructure. In 2020, children in the state of Mecklenburg-Western Pomerania began their summer holiday on June 20, whereas children in Baden Wurttemberg had to wait a further six weeks, until July 30. Similarly, the fall holidays, which are typically two weeks long, started on October 3 in the states of Schleswig-Holstein children and Hesse, but only on October 24 and 31 in the states of Baden Wurttemberg and Bavaria. We exploit this quasi-experimental variation using an estimator developed by Borusyak et al. (2020) for difference-in-differences settings with staggered adoption of treatment and heterogeneous treatment effects, which offers advantageous robustness and efficiency properties.

Two features of the German summer and fall holidays make them attractive as the source of causal identification. First, whether the holiday starts early or late in each state is decided upon years

[2] These estimates were computed on our own with data described in Section 2.2, as of October 26, 2020. To date, it is unclear whether the under-representation of children among confirmed cases is related to a higher probability of an asymptomatic course of disease, lowering the number of recorded cases, or a lower susceptibility to infection.

[3] A "closed cohort study" of a high school in France that was among the first to report a COVID-19 case reported high infection rates among pupils (Fontanet et al. 2020); a larger-scale study in schools in and around Dresden, Germany, suggested a low prevalence of antibodies and lower susceptibility to infections (Berner 2020). A third study from Trento, Italy using contact tracing found that children under 15 years were the most contagious of any age group (Fateh-Moghadam et al. 2020, with a sample size of 14).

[4] An alternative to the "cohort studies" is to examine the viral concentration in the upper respiratory tract in test samples. Most such studies published in the course of the summer 2020 found no evidence of a smaller viral load in children than in infected adults (Heald-Sargent et al. 2020; Jones et al. 2020). Viral concentration studies come with a host of caveats, one of which is sample selection. Symptomatic subjects may be overrepresented in the clinical samples of tests studied, making it difficult to draw inferences on a population of children with a large share of asymptomatic cases.

in advance and was unaltered by the pandemic. Therefore, the variation in the start and end date of the holidays across German states was not confounded by the spread of SARS-CoV-2 in the state. Second, in contrast to school closures during the first lockdown in March, the start and end of summer school holidays did not coincide with the introduction of other containment measures, such as the closing of bars, restaurants and non-essential shops, allowing us to isolate the impact of school closures. This was also the case for the fall holiday, with the exception of a partial lockdown[5] announced at the federal level implemented November 2, which is why we focus on the fall holiday closures and restrict the empirical analysis to the period preceding the lockdown announcement, October 28.[6]

Difference-in-differences estimation of the effects of schools on the spread of SARS-CoV-2 at the regional level is also attractive from a policy perspective. These estimates identify an overall impact, encompassing all behavioural adjustments that school closures bring about, such as increased activities of children outside school and reduced work-related contacts of parents. Moreover, the baseline against which school closures are evaluated is not the status quo before the pandemic, but a situation in which various other containment measures are in place. By analysing the effects of both school closures and reopenings, we evaluate whether schools that operated at partial capacity (as it was the case before the summer holiday) play a more limited role in spreading SARS-CoV-2 than schools that reopened to full capacity, with additional hygiene rules and other restrictions, at the end of the summer holiday. By comparing the effects of the summer and fall holiday closures, we assess whether closures are more effective at containing the spread of SARS-CoV-2 in situations when cases in the population are high (as in the fall) compared to situations when they are low (as in the summer). Our estimates are, therefore, directly informative on the trade-offs that policymakers may face in the future.

At the same time, some limitations of our methodology are worth pointing out. The summer holidays are a time of increased travel for families. Most likely, this increased the risk of infection, especially since the infection rates in typical destination regions were higher than in Germany. With our strategy, it is challenging to disentangle any rise in confirmed COVID-19 cases due to travel from a rise due to school reopenings *per se*. Moreover, Germany started testing travel returnees, including children, at an increasing rate starting August 1, potentially raising the number of positive cases even without a true increase in the infection rate. To tackle this difficulty, we leverage the exact timing of

[5] The lockdown implemented November 2 involves closures of cultural entertainment venues, restaurants, pubs and bars. Schools or day care centers were set to remain open.
[6] By October 28, the fall holidays have ended in most states with the exception of Thuringia, Saxony, Baden Wuerttemberg and Bavaria.

the increases in cases around the date of reopening after the summer holiday to determine the most likely explanation. While the fall holidays are less likely to be contaminated by travel behavior (since families travel considerably less during the fall than the summer), their short duration and more limited cross-state variation in timing prevent us from considering fall school closures and reopenings as separate events.

We find little evidence that school closures in the summer lowered SARS-CoV-2 infection rates among school-aged children or elder generations. At best, according to the lower bound of the 95% confidence interval of our baseline estimates, only 0.33 infections per 100,000 school-aged children (ages 5-14) and 0.03 infections per 100,000 adults aged 60 and above have been prevented per day in the first three weeks of the school summer holiday.

Similarly, we don't find that the return to full-time schooling after the summer holiday led to an increase in infections among school-aged children. Instead, we find that SARS-CoV-2 infection rates tend to increase in the last weeks of the summer holiday and decline in the first days after schools open, a pattern visible in all age groups, but more pronounced in the younger population. We consider this to be best explained by an increase in testing of families returning home from their travels or the higher risk of infection they are exposed to while travelling. It could, however, also be attributed to precautionary testing before the start of the school term.

Our findings based on the fall holiday confirm that school closures do not significantly reduce COVID-19 cases among either children or adults, even in situations when COVID-19 cases in the population are higher. These results are, however, limited to two weeks after the start of the holiday and therefore may not capture spillover effects that take longer to appear; they are also less precisely estimated.

Our results are broadly in line with contemporaneous work by Isphording et al. (2020), who use a similar research design to estimate the impact of school reopenings after the end of the German summer holiday. Two differences are worth noting, however. While their analysis exclusively focuses on the reopening of schools at the end of the summer holiday, we evaluate school closures and reopenings in the summer as separate events and provide complementary evidence on the closures induced by the fall holiday. In addition, we pay extra attention to the period just before schools reopened in the summer and identify a significant increase in infection rates during that time. This leads us to conclude that travel returnees may have contributed to the spread of SARS-CoV-2.

At the same time, our findings differ from those of Adda (2016) who found that school holidays reduce the incidence of viral diseases such as gastro-enteritis and influenza among both children and adults. One explanation for the difference in findings could lie in the differences between SARS-CoV-2 and other viruses. Alternatively, the difference could stem from the hygiene rules and

procedures currently in place in schools to avoid contagion, which are not typically implemented during the seasonal outbreaks of other diseases studied by Adda (2016).

Overall, our findings cast doubt on the assumption that school closures are successful at reducing the spread of SARS-CoV-2 in the population. Our results also provide little support for the hypothesis that school openings at the start of the academic year substantially contributed to the surge in infections observed in the fall of 2020.

The remainder of this paper is organised as follows. Section 2 provides background information on the spread of the SARS-CoV-2 virus in Germany, the containment measures implemented, school holidays, and introduces the data. The empirical strategy is described in Section 3. Section 4 reports the empirical results, and Section 5 concludes.

2 Background

2.1 The Institutional Setting in Germany

Germany's Policy Response to the Pandemic

Germany's early response to the pandemic in spring 2020 differed from its later and current response. In the German federal system, the states have large autonomy to legislate, including on matters of disease prevention. For that reason, the start of the outbreak was characterised by uncoordinated policy responses by the state governments. Independent state decisions on issues such as compulsory mask wearing in public transit and closing bars and restaurants were often timed similarly (see the see IAB database on the containment measures in Germany; Bauer and Weber, 2020). But implementation and enforcement of these policies varied from state to state.

Similar patterns characterized school closures during this early period. Drawing on the experience with influenza, where school closures proved particularly effective (Viner et al., 2020; Adda 2016), schools were closed early in the outbreak of SARS-CoV-2, around March 16. After the Easter holidays (around April 18), all states proceeded to partially reopen schools, although not for all cohorts and not for all school types symmetrically (Frankfurter Allgemeine Zeitung, 2020). Cohorts with examinations were prioritised and shifts were introduced as a solution in many schools. It was the task of schools to gauge how best to guarantee compliance with social distancing rules and hygiene standards.

This policy environment makes the spring period unsuitable for our analysis: the variation in the timing of school closures is limited and was strategically chosen by states in response to the local dynamics of the pandemic. Moreover, other containment measures coincided with school closures.

In contrast, the summer and fall holidays happened during the period when fewer new policies were being introduced (with exceptions discussed below), and containment measures tended to be homogenous across states. The latter was a consequence of the Federal Government's coordination efforts in late spring, in order to increase policy transparency and ensure compliance. We therefore start our analysis on June 1, by which point the coordination process was largely over.

Three important policy measures were introduced during our period of study, in a homogenous way across states. First, the state governments coordinated to ensure that at the end of the summer holidays schools across Germany returned to teaching at full capacity (Handelsblatt, 2020). Second, the Federal Government ensured the testing of returning travellers across the country. On August 1, it waived the cost of testing for these returning travellers, and on August 8, it introduced compulsory testing for travellers returning from high-risk countries.[7] Third, Germany announced on October 28 and implemented on November 2 a partial nation-wide lockdown, involving closures of entertainment venues, restaurants, pubs and bars. Schools and day care centres, however, were set to remain open. This partial lockdown does not affect our analysis on the closures and reopenings in the summer but overlaps with the fall holiday in Bavaria (and marginally in three other states where the holiday ended on November 2). When analysing the impact of fall holiday closures on COVID-19 cases, we therefore restrict our analysis to infections up to October 28, the day the lockdown was announced.

The Summer and Fall School Holidays

Since our empirical strategy will exploit the variation in the start and end dates of the summer and fall holiday across the 16 German states, it is important to explain the process generating this variation. In Germany, school summer holiday dates are planned several years in advance, with most states alternating between early and late summer holiday starting dates.

Figure 1 offers an overview of the holiday start and end dates in the summer (Panel A) and fall (Panel B) of 2020. Summer holidays last six weeks in all German states. There are also six weeks between the state with the earliest and latest start of the school summer holidays. The summer holiday period stretches across almost three months, with the first schools closing on June 20 and last schools reopening on September 13. The fall holiday starts as early as October 3 in the states of Mecklenburg Western Pomerania, Schleswig-Holstein, Hesse and Hamburg and as late as October 24 and 31 in the states of Baden Wurttemberg and Bavaria. In 12 out of the 16 states, fall

[7] One state constitutes a small exception, as it had introduced these policies before the Federal Government. In Mecklenburg-Western Pomerania the summer holidays ended on August 2, and tests were made compulsory at the state level beforehand (Deutschlandfunk, 2020).

holidays last two weeks; in four states, they last one week only. States that start their summer holiday early typically also start their fall holiday early.

Figure 2 illustrates the geographic variation in the summer holiday start date, showing that summer school holidays started first in one of Germany's most Northern states (Mecklenburg Western Pomerania) and last in Germany's most Southern states (Baden Wurttemberg and Bavaria).

The fall holidays are of independent interest to study for two reasons. First, because they fell into a period when infection rates were considerably higher than during the summer holidays and when the effectiveness of school closures in containing the spread of SARS-CoV-2 may thus have been higher. Second, because two week-long school closures have been discussed as possible "circuit breakers" in for example England (The Telegraph, 2020). Despite their relevance, the fall holiday setting has important drawbacks. Because of their short duration and the more limited cross-state variation in start dates, we can reliably estimate the effects of fall school closures on the spread of SARS-CoV-2 only up to two weeks since the start of the fall holiday and, even over this time period, estimates are less precise than for summer school closures and reopenings.

2.2 Data

This paper relies on data from the federal government agency known as the Robert Koch Institute (RKI), which is responsible for the prevention and control of epidemics in Germany, as well as for epidemiological research. Their database has recorded all confirmed positive cases, deaths and recoveries in Germany on a daily basis since the first COVID-19 case was reported on January 15, 2020.[8] In our descriptive and empirical analysis, we use data up until October 28. The data are available at the county ("Landkreis") or city ("Stadtkreis") level. Berlin constitutes an exception, where the data are available by borough ("Bezirk"). Altogether, the dataset comprises 415 regional entities which we refer to as districts.

Each positive case is coded with a "reporting date" when it became known to the local health department, which is generally the same day the test results were received.[9] All positive cases are either (i) confirmed recovered, (ii) deceased or (iii) neither recovered nor deceased when they are still under quarantine restrictions. This information allows us to obtain the number of deaths at the regional level. The deaths are coded according to the reporting date, the day on which

[8] Retrieved on November 14, 2020, from:
https://www.arcgis.com/home/item.html?id=f10774f1c63e40168479a1feb6c7ca74.
[9] Source: RKI, phone interview. For around 60% of cases a "reference" date is also provided, when the first symptoms appear. However, due to a large fraction of missing data (in particular, because of asymptomatic cases), we do not use these reference dates in the analysis.

the deceased person tested positive for the virus, and not the day of death. In addition, the data contain information regarding age brackets for each case, classified as 0–4, 5–14, 15–34, 35–59, 60–79 and over 80-years-old.

Positive cases are registered in the district in which the person is staying on the reporting date and where the quarantine regulation is enforced. The district to which a positive case is attributed does not, therefore, necessarily correspond to the place of residence. However, it is to be expected that the wide majority returning from travels get tested in their place of residency.[10]

From a list of confirmed reported cases, we transform the data into a daily panel dataset. We then augment it to include population counts by age brackets which were retrieved from the regional database ("Regionaldatenbank") and correspond to December 31, 2018.[11] For the boroughs of Berlin, the data were instead obtained from the Statistical Office of Brandenburg-Berlin as of December 31, 2019.[12]

2.3 A Descriptive Outlook on the Spread of SARS-CoV-2 in Germany

Before proceeding to the analysis, we provide an overview of the dynamics of the SARS-CoV-2 spread in Germany. Figure 3 contrasts daily cases (Panel A) and daily deaths (Panel B) per 100,000 inhabitants in Germany (red line), the United States (purple line) as well as four selected European countries (France, Italy, Sweden and the United Kingdom), based on the data from the European Centre for Disease Prevention and Control (ECDC).

In Germany, the peak of daily cases in the first wave of infections was reached on the March 28, 2020, with 7.51 reported cases per 100,000 inhabitants (6,294 overall), and the peak of daily deaths on April 16 with 0.38 deaths per 100,000 (315 overall).[13] Daily cases remained relatively low – fewer than one reported case per 100,000 – throughout May and June when lockdown measures were gradually eased. Since late-July, reported cases have been steadily increasing, with a noticeable uptick in cases in early October. For the first time on October 15, the ECDC reported more cases per 100,000 than at the peak of the first wave (7.92 per 100,000; 6,638 overall).

By international comparison, Germany showed a similar trend in newly reported cases as other European countries such as Italy, France and the United Kingdom between March and June.

[10] Information received via email exchange with the Robert Koch Institute.
[11] Retrieved from: https://www.regionalstatistik.de/genesis/online?language=de&sequenz=tabelleAufbau&selectionname=12411-04-02-4
[12] Retrieved from: https://www.statistik-berlin-brandenburg.de/datenbank/inhalt-datenbank.asp
[13] These numbers use the data from the European Centre for Disease Prevention and Control (ECDC). According to the RKI database (which our empirical analysis relies on), the peak of daily new cases and daily new deaths were both reached on the April 2, 2020, with 7.88 reported cases per 100,000 inhabitants (6553 overall) and 0.50 deaths per 100,000 (415 overall). Note that the RKI database reports the date the deceased person was reported positive, and not the date of death.

While most European countries experienced an acceleration in daily reported cases during the autumn, the increase has been less pronounced in Germany than in France, the United Kingdom, and Italy. The United States followed a different time pattern, in that new cases per 100,000 never fell below 9 per day, reached a first peak of about 20 in late July, and started increasing again in September, albeit at a slower pace than in most European countries.

Relative to other countries, Germany stands out in terms of the relatively low death toll. At the peak of the first wave, the death rate per 100,000 inhabitants was about 0.38 (315 overall) in Germany, but above 1 in Italy, France, the United Kingdom and Sweden. While the second wave of the pandemic has turned out to be less deadly than the first wave, an uptick in daily deaths per 100,000 inhabitants starting in early October is clearly visible in the United Kingdom, France and Italy, and to a lesser extent in Germany. In Germany, and likewise for other countries, adults aged 60 and above have a considerably higher risk of dying from the COVID-19 disease and make up 95% of all deaths.

Figure 4 shows daily SARS-CoV-2 cases per 100,000 over time by six age brackets. Strikingly, during the first wave of the pandemic in March and April —when, for the most part, schools were closed due to general lockdown measures—infection rates among children (aged 14 and below) were low, both in absolute terms and relative to other age groups. In contrast, during the "second wave" of the pandemic in September and October—when schools were open—infection rates among children rose at a similar pace to those of adults. The increasing share of children among newly confirmed cases appears to coincide with the end of the summer school holiday and has been linked to school openings by the press (New York Times, 2020; ZEIT, 2020). The quasi-experimental variation in the school holiday dates in Germany offers a unique setting to investigate that relationship in a rigorous manner.

3 Methodology

Identifying the impact of school closures and openings on the spread of SARS-CoV-2 using modern econometric tools is complicated for several reasons. School closures and openings are typically enforced nation-wide, making it impossible to disentangle these effects from general time trends. Moreover, when there is variation in school closures across regions within the same country, it typically results from the regional responses to rising infection rates and hence cannot plausibly be considered unconfounded. A similar problem arises in studies that exploit variation in the timing of school closures and openings across countries; such studies are additionally plagued by differences in the testing procedures of these countries.

In addition, school closures and openings typically go hand in hand with the introduction

and easing of other lockdown measures, making it impossible to isolate the impact of school closures and openings on SARS-CoV-2 infection rates. For example, when schools were closed country-wide in Germany in March 2020, all non-essential shops, including bars, were also closed, travel restrictions were expanded, workers were told to work from home wherever possible, and simultaneously limitations on contact between households were introduced.

To overcome these identification challenges, we build on Adda (2016) and exploit the variation in the timing of summer and fall school holidays across German states to isolate the impact of school closures and reopenings from other factors on the spread of SARS-CoV-2. As outlined in Section 2.1, the schedule of school holidays in 2020 was unaltered by the pandemic and did not coincide with other state-specific lockdown measures. The German setting is particularly interesting in this context, since, as also explained in Section 2.1, the variation in the timing of both summer and, to a smaller extent, fall school holidays is larger than in other countries.

For identification, we rely on a difference-in-differences design with staggered adoption of treatment. This methodology assumes that the true causal model for the outcome of interest reported in district i on day t is

$$Y_{it} = \alpha_i + \beta_t + \tau_{it} D_{it} + \varepsilon_{it}. \quad (1)$$

Here α_i and β_t capture the district and day fixed effects and $D_{it} = 1[t \geq E_i]$ is the indicator that the district is "treated" (i.e., schools have closed or reopened, depending on the analysis), where E_i is the day when district i is treated. We separately consider two treatments: school closures and openings in the summer and the closures in the fall. Further, τ_{it} captures the "treatment effect"—that is, the impact of the school closures and openings on the spread of SARS-CoV-2—while ε_{it} is the residual such that $E[\, \varepsilon_{it} \mid \alpha_i, \beta_t, D_{it} \,] = 0$. The model in (1) incorporates the parallel trends assumption, whereby the expected outcome absent the treatment is $\alpha_i + \beta_t$. It also allows for heterogeneous treatment effects by district and time, and thus by the number of days since treatment.

To characterize treatment effects, we use the "imputation estimator" of Borusyak et al. (2020). A recent literature has shown that estimating equation (1) as a conventional event study, i.e. by OLS with two-way fixed effects and some lags and leads of treatment, produces estimates that are not reliable in presence of effect heterogeneity and potentially even have a wrong sign. Several robust estimators have been recently proposed (e.g., de Chaisemartin and D'Haultfœuille 2020; Sun and Abraham 2020). Relative to these estimators, the imputation estimator possesses attractive efficiency properties, is transparent, and conservative standard errors are available for it, which can be computed analytically.[14]

[14] We implement the analysis using the *did_imputation* Stata command provided by Borusyak et al. (2020).

The imputation estimator is constructed in three steps. First, the district and day fixed effects α_i and β_t in equation (1) are estimated by OLS on the subsample of untreated observations only, i.e. those with $D_{it} = 0$. In the case of the school closures we, therefore, estimate α_i and β_t using the data until the last day of school before the start of the holiday in each state. Second, we obtain an unbiased estimate $\hat{\tau}_{it} = Y_{it} - \hat{\alpha}_i - \hat{\beta}_t$ for each treated observation. While treatment effects for each day and district cannot be estimated consistently, Borusyak et al. (2020) show that averages of $\hat{\tau}_{it}$ across many observations can, under appropriate regularity conditions. Any such average of interest can therefore be reported in the third step. We focus here on the average effect a given number h days since treatment ($h \geq 0$):

$$\hat{\tau}_h = \frac{1}{|I_h|} \sum_{i \in I_h} \hat{\tau}_{i,E_i+h}\,, \tag{2}$$

where I_h is the set of districts i observed in period $E_i + h$.

For each horizon h, the imputation estimator leverages all difference-in-differences contrasts between some district i in period $E_i + h$ (i.e., on a day h days after treatment) relative to periods before treatment, $t < E_i$, and relative to other districts which have not been treated yet by $E_i + h$. This estimator is only available for $h < H$, where H is the gap between the earliest and latest event dates observed in the sample (six weeks in our case, or five weeks with a reasonable sample size). This is in contrast to OLS estimates which are in principle possible to estimate for any long horizons but may not be reliable: there are no difference-in-differences contrasts that can directly identify those effects, and the estimates are obtained solely by extrapolations appropriate only under constant treatment effects. We focus on the effects of the school closures and openings in the summer up to three weeks after the beginning and end of the summer holiday (i.e., for $h = 0, \ldots, 20$).

In our baseline specification, we define the outcome variable Y_{it} as the number of confirmed COVID-19 cases per 100,000 inhabitants in some age bracket. We distinguish between children aged from 5 to 14 years old, whose infection risks may be directly reduced by school closures, and adults, for whom the effects are indirect. Limited by our data, we consider three adult age groups: a group of young adults between 15 and 34 years old; a group of middle-aged adults between 35 and 59 years old, in which most parents of school-aged children will fall; and a group of vulnerable adults older than 60 years of age. We also consider the number deaths per 100,000 inhabitants in the 60+ age group, since 95% of the deaths are concentrated in that group.

We start out by estimating the effects of the school closures in the summer on the spread of SARS-CoV-2. To provide empirical support for the assumption of parallel trends, we follow Borusyak et al. (2020) and estimate the regression on the set of untreated observations only:

$$Y_{it} = \alpha_i + \beta_t + \sum_{p=-P}^{-1} \gamma_p 1[t = E_i + p] + \varepsilon_{it}. \quad (3)$$

Here, $1[t = E_i + p]$ are indicator variables of being treated 1 to P days later; we set $P = 14$. A conventional joint test of $\gamma_p = 0$ is then performed, and the magnitude of $\hat{\gamma}_p$ can be visually examined. It is important to note that this approach for pre-trend testing differs from the convention where pre-trend or placebo coefficients are estimated jointly with the treatment effects $\hat{\tau}_h$. Borusyak et al. (2020) explain three advantages of this approach. First, it clearly separates validation of the design (i.e. of the ex-ante assumption of parallel trends) from estimation given the design. Second, by imposing no pre-trends at the estimation stage, it improves efficiency of treatment effect estimation: all untreated observations are used in the imputation. Third, it removes the correlation between the treatment effect and the pre-trend estimators; such correlation introduces bias when the researcher follows the conventional practice of trusting the results only conditionally on the pre-trend test passing.

When turning to the effects of school reopenings in the summer, we additionally allow for "anticipatory" effects of treatment present up to K days before treatment; we set $K = 14$. We do this to allow for the possibility that SARS-CoV-2 infection rates may increase prior to school openings because of travel returnees and increased testing. Families often return home in the last two weeks of the summer holiday and, as described in Section 2.1, typically spend their vacation in regions where infection rates were higher than in Germany and were tested upon returning home. The imputation estimator extends directly to the case of anticipation effects, with the treatment indicator redefined to switch to one K days before treatment: $D_{it} = 1\ [t \geq E_i - K]$. We (re)estimate district and day fixed effects α_i and β_t in equation (1) using only those observations that are assumed to be unaffected by the school opening treatment (i.e., observations more than two weeks before the end of the summer school holiday). We also check for "pre-trends" in a similar way as for school closures, by estimating equation (3) on a set of untreated observations and by testing whether the γ_p coefficients are individually and jointly equal to zero.

It should be noted that, when examining the effects of school reopenings on the spread of SARS-CoV-2, we implicitly assume that the preceding school closures in the summer have had no impact on SARS-CoV-2 infection rates. We explicitly investigate—and provide empirical support for—this assumption in the first part of the empirical analysis, where we study the effects of summer school closures on the spread of SARS-CoV-2.

In the final step of the empirical analysis, we estimate the effects of fall holiday closures on the spread of SARS-CoV-2. We consider anticipatory effects due to travelling behavior unlikely in this context and therefore test for differential pre-trends in the 14 days prior to the start of the school

holiday (i.e., we set $K = 0$ and $P = 14$). As Panel B of Figure 2 shows, the difference in the start dates of the fall holidays between states that introduced them first and last is four weeks (compared to six weeks for the summer holidays), so that we could in principle estimate the effects of fall school closures up to four weeks since the start of the fall holiday. However, the state in which fall holidays started latest (Bavaria) appears to exhibit a different time trend in infection rates from other states and thus is not a reliable control group. Hence, estimates for the impact of fall school closures on the spread of SARS-CoV-2 beyond the first two weeks rest on a single state (Baden Wuerttemberg). We therefore focus in our analysis on effects in the first two weeks after the start of the fall holiday and do not consider fall school closures and reopenings as separate events.

In the appendix, we examine the robustness of our main empirical strategy with two alternative ones. First, we adopt the conventional event study methodology, which involves estimating the following equation via OLS:

$$Y_{it} = \alpha_i + \beta_t + \sum_{h=-K}^{H-1} \tau_h 1[t = E_i + h] + \varepsilon_{it}. \quad (4)$$

Here K is the number of treatment leads, corresponding to the allowed anticipation effects, and the effects K or more days before treatment are assumed to be zero. Focusing on the effects in the first H days after treatment, we drop observations with $t \geq E_i + H$ (which is preferable to the common alternative of "binning" them together; see Borusyak et al., 2020).

Second, we note that parallel trends in levels may not hold if there are national trends in infection rates that affect districts proportionately rather than additively. In that case, the following multiplicative model may be more appropriate:

$$E[Y_{it} \mid \alpha_i, \beta_t] = \exp(\alpha_i + \beta_t + \tau_{it} D_{it}). \quad (5)$$

While, in principle, one could estimate a log-linear specification, it appears infeasible in our application, as there are many district-day pairs for which no COVID-19 cases were recorded. We therefore use the Poisson Pseudo-Maximum Likelihood (PPML) method, appropriate for this assumption (e.g. Santos Silva and Tenreyro, 2006), and use the PPML-HDFE estimator of Correia et al. (2020) which allows for high-dimensional fixed effects. Since robustness of PPML methods to treatment effect heterogeneity has not been studied to date, and since robust estimators are not available, we use the event study formulation analogous to (4).

4 Empirical Findings and Discussion

4.1 The Effect of Summer School Closures on the Spread of SARS-CoV-2

The Impact of School Closures on Infection Rates among Children.

We begin by examining the impact of the school closures induced by the summer holidays on infection rates among school-aged children. In Panel A of Figure 5, we group states into six categories according to their school summer holiday start date, ranging from June 20 (red line) to July 30 (black line), and display COVID-19 cases per 100,000 children, smoothed using a moving average filter with three lags and three leads, from June 1 until schools reopen at the end of the holiday. The colored vertical lines indicate the respective starts of the summer holiday. The infection rates among children remained relatively constant in the three weeks leading up to the summer holiday, as well as the first three weeks of holiday. Panel A therefore already provides little descriptive evidence to support the hypothesis that school closures helped bring down rates of infection among children. In Panel B of Figure 5, we plot "placebo" estimates prior to treatment obtained from regression equation (3) (the red squares) and "treatment" effects for three weeks following school closures, estimated according to equation (2) (the blue dots), together with 95% confidence intervals. The figure validates the empirical design: the pre-trend coefficients are small and, with one exception, statistically insignificant.[15] Moreover, the figure confirms the pattern observed in Panel A, namely that the school closures have had little impact on infection rates: the treatment effects are small and typically statistically indistinguishable from zero.

We report the corresponding treatment effects averaged over the first three weeks of the summer holiday in the first row of Table 1. The point estimate for the entire three-week period is -0.12 (column (4)), with a 95% confidence interval of [-0.33, 0.09]. Thus, taking the uncertainty of the estimate into account, the lower bound of the confidence interval implies that the school closures have – at best – prevented 0.33 infections per 100,000 children daily. This is a rather small effect in terms of absolute magnitude. It should be noted, however, that the mean daily infection rate of children in the week before the start of the summer holiday was also very low (0.68, see column 5 of Table 1).

The Impact of School Closures on Infection Rates among Adults.

Next, we turn to the impact of the school closures on SARS-CoV-2 infection rates among adults, where we distinguish between adults in the age ranges of 15-34, 35-59, and 60+. Figure 6

[15] It should be noted that the F-test weakly rejects the hypothesis that coefficients are jointly equal to zero with a p-value of 0.011. However, coefficients are sometimes below and sometimes above zero and do not exhibit a clear upward or downward trend.

repeats the structure of Figure 5 for each of these groups, with rows (2) to (4) of Table 1 providing the corresponding averages. Overall, they provide little support for the hypothesis that school closures would help bring down infection rates. For example, the lower bound of the confidence interval for the most vulnerable group of adults – the population older than 60 (row (4) and column (4) in Table 1) – signifies that school closures prevented at most 0.025 infections per 100,000 per day in this group.

In Figure 7 and in row (5) of Table 1, we repeat the analysis of deaths per 100,000. Here, we restrict the analysis to adults aged 60 and above, the age category comprising 95% of all COVID-19 deaths in Germany. Not surprisingly, given our previous findings, there is no indication the closures helped prevent deaths.

To summarize, the summer closures appear to have had little impact on SARS-CoV-2 infections among children and adults. These results are robust to alternative estimation methods such as the conventional event study (Appendix Figure A1) and PPML (Appendix Figure A2). To put these results into perspective, it is important to bear in mind that schools typically operated at only half capacity before the summer holiday. Moreover, in the weeks before the start of the school holiday, SARS-CoV-2 infection rates were generally low in all states, with an incidence of around 0.7 per 100,000 inhabitants per day. In such a situation, it may not be surprising that school closures in the summer did not help reduce the infection rate further.

4.2 The Effect of School Reopenings after the Summer Holidays on the Spread of SARS-CoV-2

Having established that the school closures in the summer have had little impact on the spread of SARS-CoV-2, we turn to the impact of school reopenings on infection rates. After the summer holiday, schools generally started to operate at full capacity, although strict hygiene rules and clear procedures specifying what to do in the event of a school outbreak were introduced. The effects of the school closures and reopenings are therefore unlikely to be negatively symmetric. Moreover, there may be "anticipation" effects of school reopenings at play, driven by increased testing upon return from travels or precautionary testing before the start of term.

The Impact of School Reopening on Infection Rates among Children.

In Panel A of Figure 8, we display daily infection rates per 100,000 children, smoothed using a moving average filter with three lags and three leads, from June 1 to October 5 (or until the fall school holiday started, whichever is earlier). The figure distinguishes between six groups of

states with differing school reopening dates, indicated by the colored vertical lines. A striking pattern emerges. Infection rates among children tend to increase in the two weeks before the end of the summer holiday and decline shortly after schools have reopened.

We report treatment estimates based on the imputation method by Borusyak et al. (2020) in Panel B of Figure 8, where we allow for two weeks of "anticipation effects" of school reopenings (blue dots). The estimates confirm the pattern visible in Panel A: Point estimates increase and are statistically different from zero in the last two weeks of the summer holiday; they then decline from the third day of schools being open and turn negative from the second week. "Placebo" estimates prior to two weeks before schools reopened (red squares) are generally small in magnitude and not statistically significant different from zero – in line with our findings that the school closures in the summer had little impact on the spread of the SARS-CoV-2 virus in the child population.[16] The pattern of increased infections before schools reopened, followed by a decline in cases after schools reopened, is robust to alternative estimation procedures: the conventional event study (Appendix Figure A3, Panel A) and PPML (Appendix Figure A4, Panel A).

While the significant negative effects in the second and third weeks after school reopenings may appear puzzling, we do not place much emphasis on this finding. The negative effects stem from the two states which reopened their schools last (Baden Wuerttemberg and Bavaria, the purple and black lines in Panel A of Figure 8), where cases seem to have increased four weeks before the end of the holiday rather than two.[17] Removing these two states from our sample in Panel C of Figure 8 causes the negative effect to disappear and allows us to confirm the increase in cases before reopening, which dissipates shortly after.[18]

The fact that SARS-CoV-2 infection rates among children start to increase *before* schools reopen makes it highly unlikely that increased contact with other children, caused by the reopening of schools, is responsible for the uptick in cases among children. In our view, the most plausible explanation for the pattern of treatment effects relates to travel behavior. Families often spend their summer holiday in areas where infection rates were higher than in Germany. Family members, including children, were then tested at much higher rates upon returning to Germany, typically during the last two weeks of the summer holiday.

We report corresponding treatment effects, averaged over one-week periods starting from

[16] It should be noted, however, that the F-test rejects the hypothesis that coefficients are jointly equal to zero with a p-value of 0.005, which is in part related to the patterns for late-treated states described below. Note that coefficients are sometimes below and sometimes above zero and do not exhibit a clear upward or downward trend.

[17] One reason for why Bavaria and Baden Wuerttemberg could exhibit different patterns than the other states is that they are typical destinations for domestic travel by Germans.

[18] Removing these states from our sample reduces the time horizon over which treatment effects can be reliably estimated, which is why we present treatment effects only up to 10 days before and after treatment.

two weeks before and until three weeks after the end of the summer holiday, in row (1) of Table 2. Columns (4) and (5) report the average daily coefficients in the second and third week after school start – by which the temporary increase due to travel behavior and increased testing should have subsided. These estimates provide no support for the conjecture that school reopenings increase the risk of infection among children (because of increased contact with other children or for other reasons).

The Impact of School Reopenings on Infection Rates among Adults.

In Figure 9 we repeat the analysis for the three age groups of adults and obtain broadly similar results. The raw data displayed in Panel A shows upticks in confirmed cases before school reopenings, followed by a decline in confirmed cases during the first days of school. This could be related to increased testing upon return from travels or a higher risk of infection during travels. This pattern is particularly visible for states in which summer holidays ended and schools reopened early (e.g., the yellow and red lines in the figure). The estimates in Panel B of Figure 9, as well as their averages reported in rows (2) to (4) of Table 2, also show no evidence for the hypothesis that school reopenings could increase SARS-CoV-2 infection rates among adults. This conclusion is corroborated by estimates from a conventional event study (Appendix Figure A3) as well as by estimates from PPML regressions (Appendix Figure A4).

In contrast to the raw data displayed in Panel A of Figure 9, and the evidence presented for children in Figure 8, estimates in Panel B of Figure 9 capture only the negative effects on confirmed cases following the reopening of schools, but not the preceding increase in cases. When we remove the two states that reopened schools last (the black and purple lines in Panel A), like in Panel C of Figure 8, estimates become notably similar to those for children: they show an "anticipatory" increase in cases and a return to the trend within a week after the schools reopened (see Figure 10). The estimated negative effects on confirmed cases among adults observed a few days after schools reopened appear to be driven by two states and hence cannot be considered as robust.

Figure 11 and row (5) of Table 2 further suggest that school reopenings did not increase COVID-19 related death rates among adults aged 60 and above. The upper bound of the confidence interval in the first three weeks after school reopenings in row (5), column (5) of Table 2 implies that daily, at most, 0.014 deaths per 100,000 older adults could have been prevented had schools remained closed.

4.3 The Effect of Fall School Closures on the Spread of SARS-CoV-2

The effectiveness of school closures as a containment measure may depend on the stage of the pandemic at which they are enforced. Analyzing the summer holidays, we found school closures to be an inadequate containment measure at low levels of aggregate infections – with an average of 0.82 new reported cases per day and per 100,000 in the period June to August. However, the possibility remains that they prove more effective in a high-infection environment. The quasi-experimental approach of this paper opens a window to test for this possibility using the fall holidays in Germany as they were also staggered across states and fell into a period of high aggregate infection levels. The second advantage the fall holidays offer is that traveling is much less prevalent during this time, both because of the government advice against it and because the vacation is substantially shorter. A disadvantage, however, is that due to their short length and the more limited variation in timing across states, we cannot reliably estimate the effects beyond two weeks from the start of the fall holiday and, even over this time period, estimates are less precise than for the summer school closures and reopenings.

The Impact of Fall School Closure on Infection Rates Among Children

In Panel A of Figure 12, we again plot the smoothed daily infection rates per 100,000 children, starting from one week after the school reopening after the summer holiday up until the end of the fall holiday (or our sample period on October 28). The figure distinguishes among five groups of states with differing school closure dates, indicated by the colored vertical lines. The figure shows no clear change in infection rates after the holiday starts in any state. A noticeable feature of the figure is that, from October 1 onwards, infection rates among children increase at a considerably faster pace in the state of Bavaria, the last state to start the fall holiday (the purple line), than in the other states. Abstracting from this outlier, the development of infection rates over time is parallel across states both preceding and during the fall holiday. Since Bavaria clearly exhibits a different trend from the other states prior to the holiday, we drop it from the remaining analysis.

In Panel B of Figure 12, we display both "placebo" estimates prior to treatment obtained from regression equation (3) (the red squares) and "treatment" effects for two weeks following school closures, estimated according to equation (2) (the blue dots). We report corresponding point estimates, averaged over a one- and two-week windows in row (1) of Table 3. The figure and table provide little support for the hypothesis that the school closures in the fall had a containing effect on the spread of SARS-CoV-2 among children. Point estimates are not significantly different from

zero. Taking the uncertainty around our point estimates into account, the lower bound of the 95% confidence interval in row (1), column (1) of the table indicates that fall school closures have prevented at most 1.29 cases per day and per 100,000 children during the first week of the holiday. This effect can be referenced against the average case rate of 4.08 (per day per 100,000) during the week before the holiday. Alternative estimation methods such as the conventional event study (Appendix Figure A5) and PPML (Appendix Figure A6) corroborate our conclusion that the school closures in the fall did not slow the spread of SARS-CoV-2 among children.

The Impact of Fall School Closure on Infection Rates Among Adults

In Figure 13, we repeat the analysis for the three groups of adults. The raw data in Panel A of the figure shows a clear uptick in cases among all adult groups that starts in all groups of states at around the same time, around October 1. No apparent shift in trends can be detected from the figure after the starts of the fall holidays across the groups of states. The treatment effects from the imputation estimator displayed in Panel B of Figure 13 and rows (2) to (4) of Table 3 reveal no significant effects on infection rates among adults. For example, the lower bound of the 95% confidence interval in column (1) and row (4) suggests that at most 0.59 cases per day and per 100,000 adults above 60 have been prevented during the first week of the fall holiday (with the mean incidence rate of 3.13 cases per day per 100,000 during the week before the holiday). Estimates based on the conventional event study (Appendix Figure A5) and PPML (Appendix Figure A6) paint a similar picture.[19]

Taking stock, the results for the fall holidays both reinforce and complement our findings from studying the summer holidays. Like for the summer holiday, we do not find school closures in the fall to have a significant containing effect. At the same time, unlike the summer, the fall was an environment with high infection rates. This suggests that school closures may not be an effective containment measure regardless of the incidence of cases – provided appropriate hygiene rules are in place, as it was the case throughout our study period.

5 Conclusion

This paper leverages the variation in timing of the summer holidays in Germany to analyse how schools contribute to the spread of the SARS-CoV-2 virus. In contrast to the survey-approach on a selection of schools, our paper takes a broader perspective and exploits quasi-experimental variation on detailed country-wide data. Specifically, we apply the novel imputation estimator by

[19] In this analysis we continue to drop Bavaria for consistency with Figure 12.

Borusyak et al. (2020) for the difference-in-differences framework with staggered adoption.

We find that schools play a subordinate role in the spread of SARS-CoV-2, suggesting that the benefits of their closures do not outweigh the costs. The summer school closures do not appear to have had a containing effect on infections in either the school population or older generations. Similarly, an analysis of the impact of fall holiday closures allows us to evaluate whether closures are more effective in more advanced stages of the pandemic. Our results suggest they are not: the fall closures do not appear to have significantly impacted infections among children and adults, although we point out that the confidence intervals for the fall estimates are wider and do not allow us to reject the possibility of sizable effects.

In line with our results on school closures, we find concerns about the return to full schooling capacity after the summer holidays to be unsubstantiated: infections among children and adults did not rise with the start of the new academic year. Instead, infections appear to increase in the last weeks of the summer holidays and *decline* in the days after reopening. This pattern is consistent with the view that travel restrictions and testing policies have an impact, although more direct evidence would be needed to reach that conclusion with confidence.

While it is not our domain of expertise to explain *why* schools appear to play a subordinate role on the spread of SARS-CoV-2, epidemiological studies hint at several potential explanations. One possibility is that the measures introduced in German schools to avoid contagion have been effective. Alternatively, children could be less susceptible to infection (Davies et al., 2020), or less contagious than adults because of the smaller exhaled air volume and higher probability of an asymptomatic course of the disease that reduces the risk of spreading the virus by coughing (Jones et al., 2020). Further epidemiological evidence on the relative role of such mechanisms would complement the policy implications of this paper.

Figures

Figure 1: School Holidays in Federal Germany

Panel A: The Summer Holidays

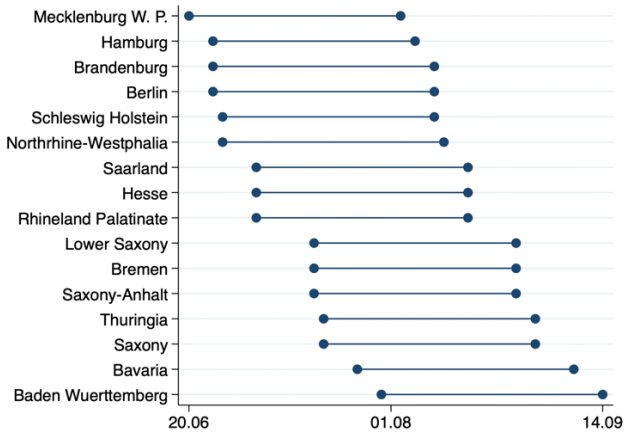

Panel B: The Fall Holidays

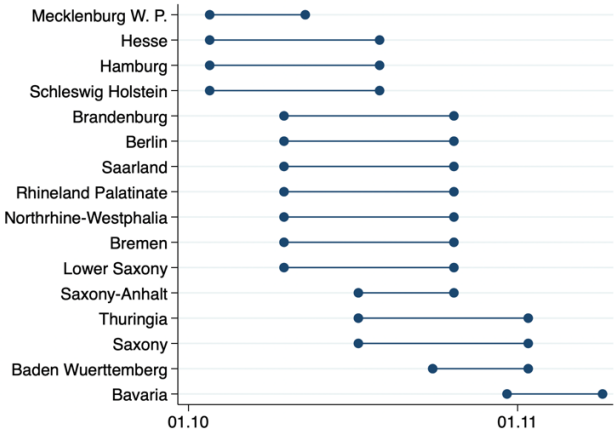

Notes: This figure displays the first day of the official school holidays in German states and the first day when schools reopened after the holiday. Panel A displays the dates for the summer holidays while Panel B the timeline for the fall holidays. We include the preceding weekend when the official holiday start falls on a Monday. The difference between the start and end dates ranges between 42 and 46 days in the summer and between 9 and 16 days in the fall.

Figure 2: Map of Germany and the Starting Dates of the Summer Holiday

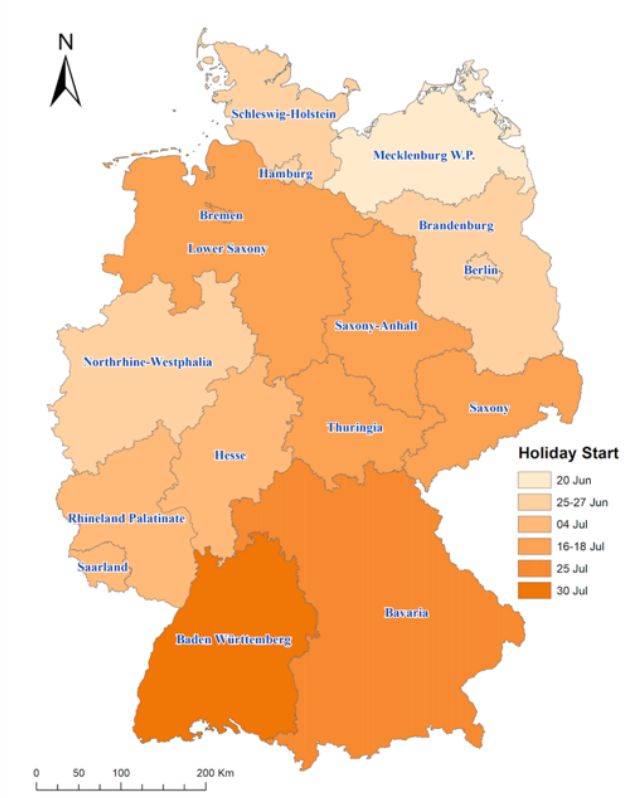

Notes: This map of Germany indicates the starting dates of the summer holiday in Germany. The colour of the state is darker, the later the start of the school holiday. Some starting dates are grouped as indicated in the legend.

Figure 3: The Course of the Pandemic: Germany in International Comparison

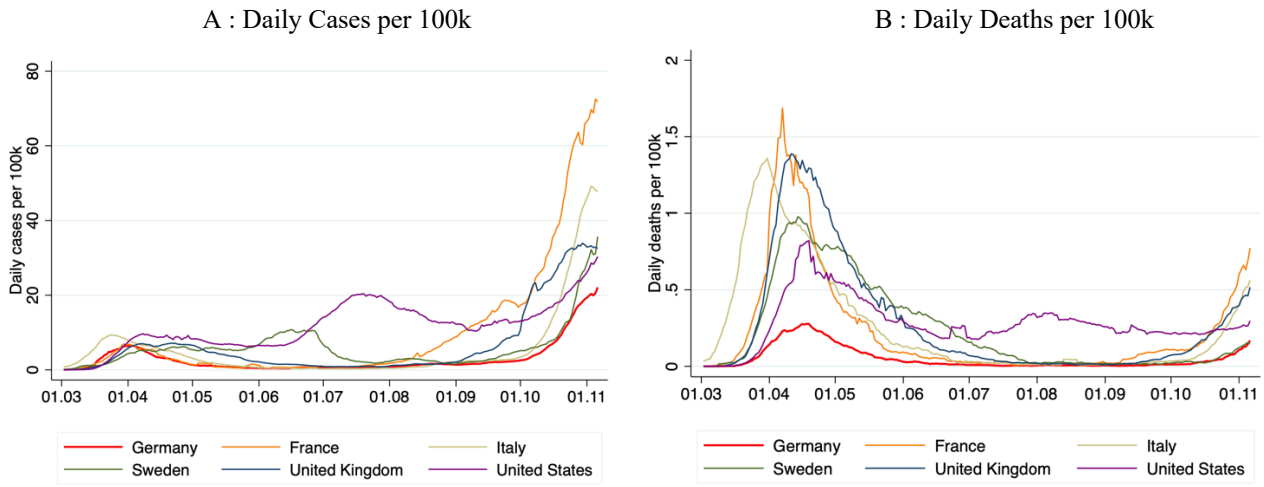

Notes: This figure displays the daily new confirmed cases (Panel A) and deaths (Panel B) per 100,000 inhabitants in Germany, France, Italy, Sweden, United Kingdom and the United States. The lines in both panels are smoothed using a uniformly weighted moving average filter with three lags and three leads. Data source (in this figure only): the European Centre for Disease Prevention and Control (ECDC).

Figure 4: SARS-CoV-2 Incidence by Age Bracket

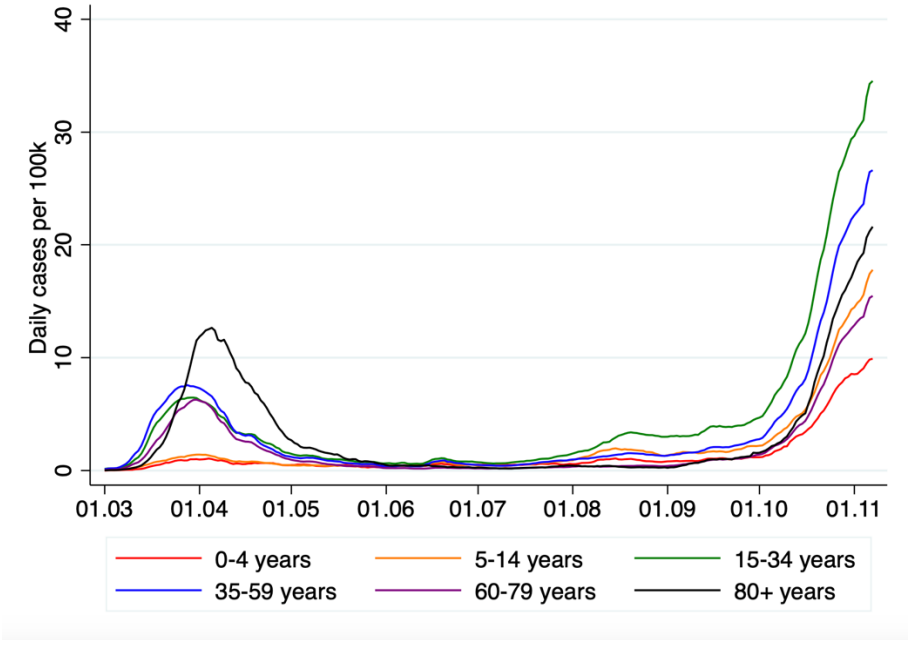

Notes: Figure 4 displays the daily new cases per 100,000 by reporting date in six available age brackets respectively: 0-4 years, 5-14 years, 15-35 years, 35-59 years, 60-79 years and 80+ years. The lines are smoothed using a uniformly weighted moving average filter with three lags and three leads. Data source: RKI.

Figure 5: The Impact of the Summer School Closures on Children of Age 5-14

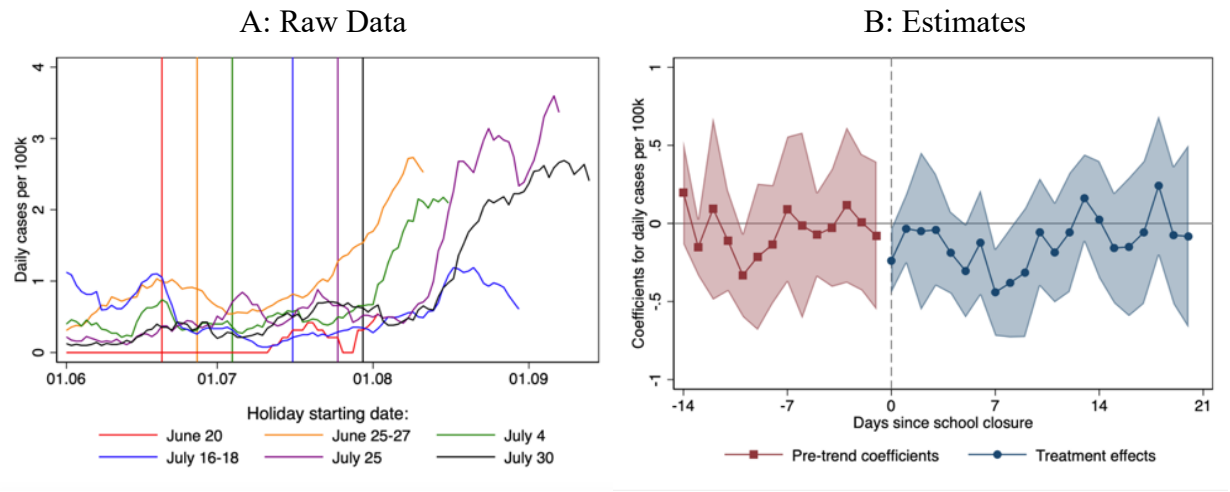

Notes: Panel A displays the daily cases per 100,000 in the age bracket 5-14 years, smoothed with a uniformly weighted moving average filter including three lags and three leads. The districts are grouped according to the holiday starting date, and the data are shown until schools reopened after the summer holiday. Panel B displays the treatment effect estimates using the Borusyak et al. (2020) imputation estimator including district and day fixed effects (blue squares, following equation (2)), as well as OLS estimates for pre-trends (red squares, following equation (3)). The outcome variable is defined as the number of daily reported COVID-19 cases (per 100,000 in the age bracket 5-14 years), and the districts are weighted according to the population in the age bracket 5-14 years. The shadows reflect the range inside the 95% coefficient interval, with standard errors clustered at the NUTS-2 level (38 clusters).

Figure 6: The Impact of the Summer School Closures on Other Age Brackets

A: Raw Data B: Estimates

Age Bracket: 15-34

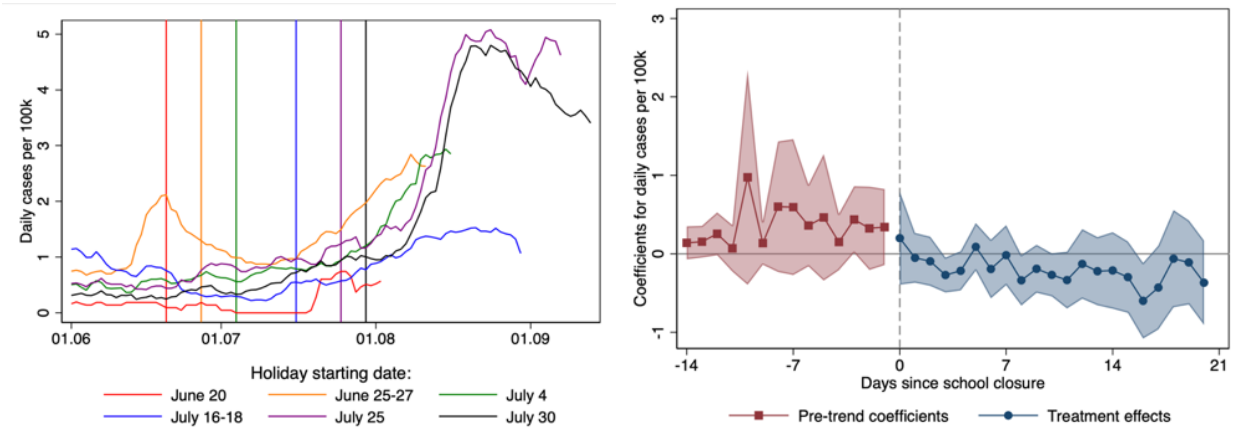

Age Bracket: 35-59

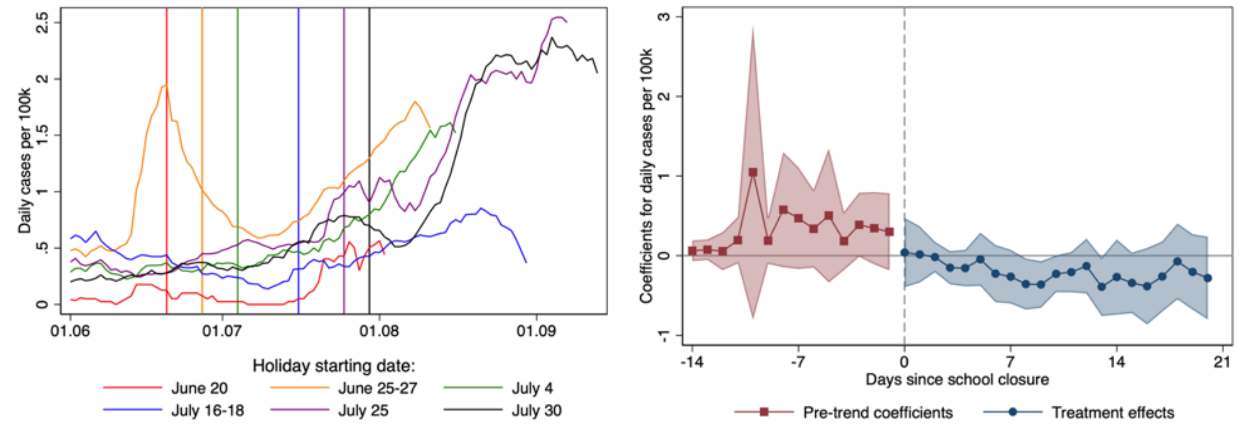

Age Bracket: 60+

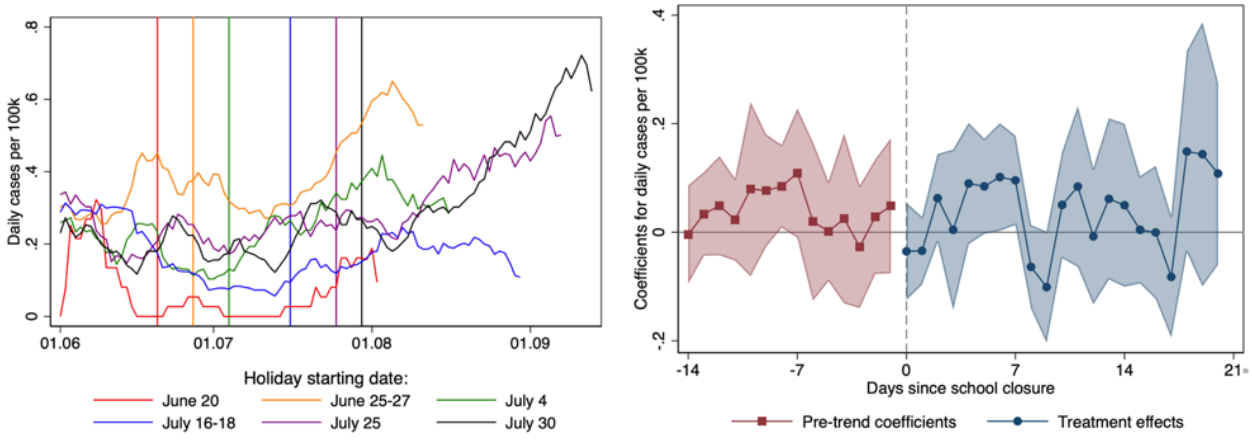

Notes: Panel A displays the daily cases per 100,000 in the respective age brackets, smoothed with a uniformly weighted moving average filter including three lags and three leads. The districts are grouped according to the holiday starting date, and the data are shown until schools reopened after the summer holiday. Panel B displays the treatment effect estimates using the Borusyak et al. (2020) imputation estimator including district and day fixed effects (blue dots, following equation (2)), as well as OLS estimates for pre-trends (red squares, following equation (3)). The outcome variable is defined as the number of daily reported COVID-19 cases (per 100,000 in the respective age bracket), and the districts are weighted according to the age-bracket specific population. The shadows reflect the range inside the 95% coefficient interval, with standard errors clustered at the NUTS-2 level (38 clusters).

Figure 7: The Impact of the Summer School Closures on Deaths, Age Group 60+

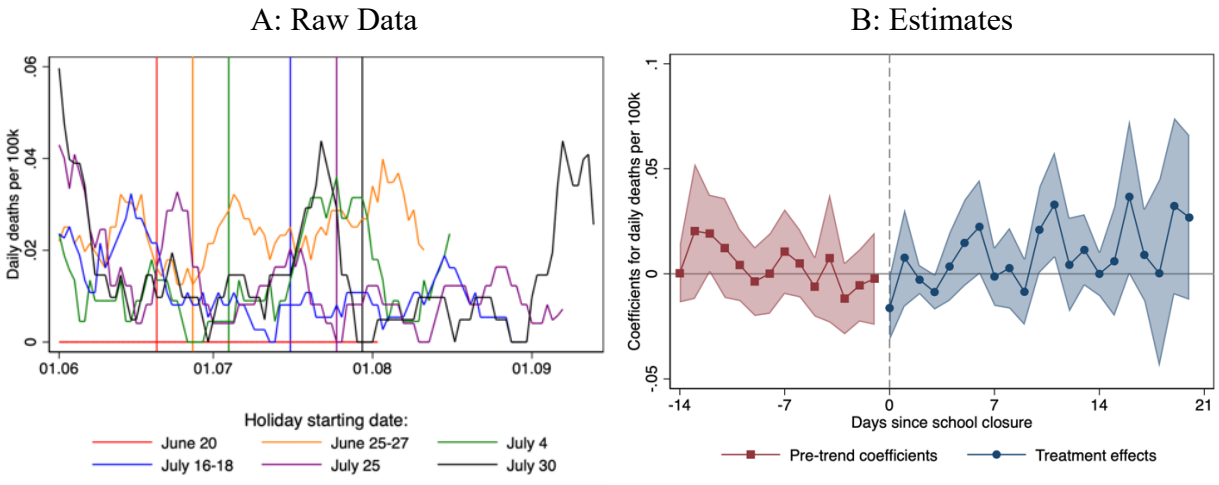

Notes: Panel A displays the daily deaths per 100,000 in the respective age brackets, smoothed with a uniformly weighted moving average filter including three lags and three leads. The districts are grouped according to the holiday starting date, and the data are shown until schools reopened after the summer holiday. Panel B displays the treatment effect estimates using the Borusyak et al. (2020) imputation estimator including district and day fixed effects (blue dots, following equation (2)), as well as OLS estimates for pre-trends (red squares, following equation (3)). The outcome variable is defined as the number of COVID-19 deaths attributed to the reporting date (per 100,000) in the age bracket 60+, and the districts are weighted according to population in the age bracket 60+. The shadows reflect the range inside the 95% coefficient interval, with standard errors clustered at the NUTS-2 level (38 clusters).

Figure 8: The Impact of the Summer School Reopenings on Children of Age 5-14

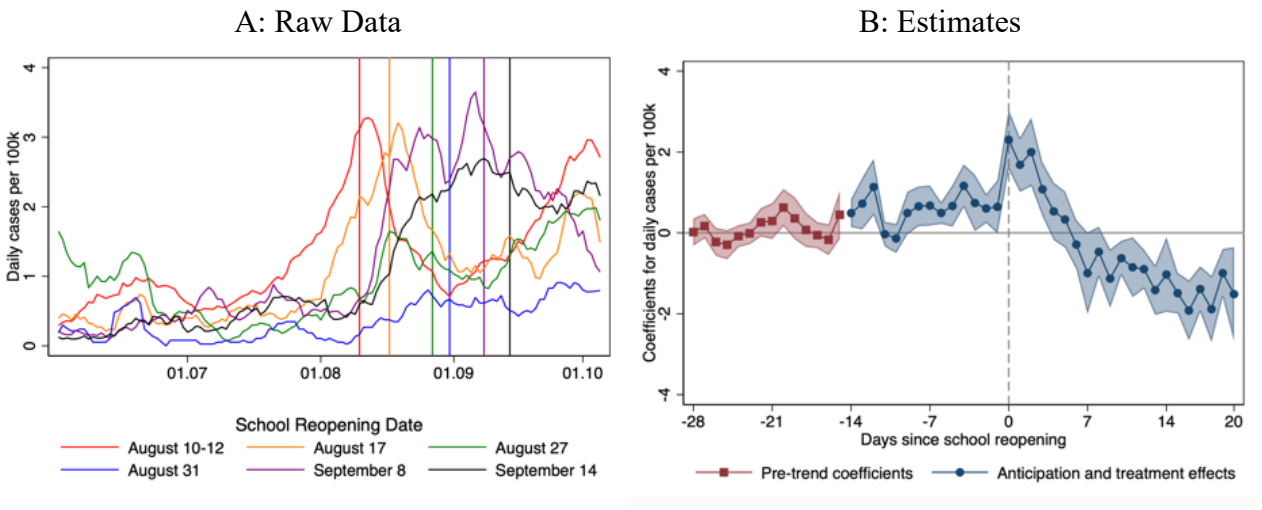

C: Estimates Dropping the Southern States

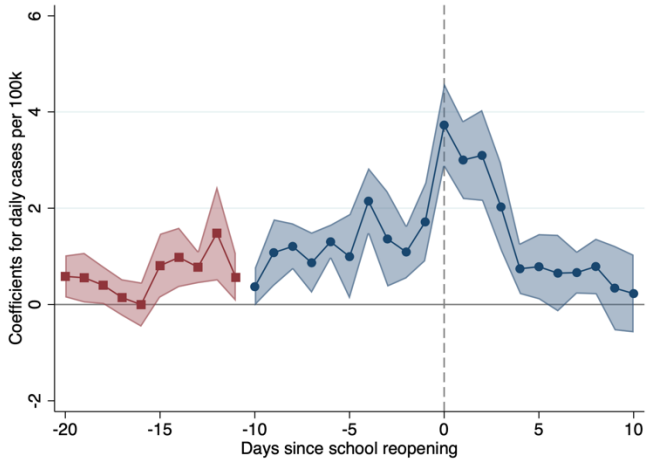

Notes: Panel A displays the daily cases per 100,000 in the age bracket 5-14 years, smoothed with a uniformly weighted moving average filter including three lags and three leads. The districts are grouped according to the school reopening date, and the data are shown until October 5 or the day when the fall holiday starts (whichever is earlier). Panel B displays the anticipation and treatment effect estimates using the Borusyak et al. (2020) imputation estimator including district and day fixed effects (blue dots, following equation (2)), as well as OLS estimates for pre-trends (red squares, following equation (3)). Anticipation effects are allowed within 14 days before schools reopened. The outcome variable is defined as the number of daily reported COVID-19 cases (per 100,000 in the age bracket 5-14 years) and the districts are weighted according to the population in the age bracket 5-14 years. The shadows reflect the range inside the 95% coefficient interval, with standard errors clustered at the NUTS-2 level (38 clusters). Panel C displays the results from the same specification as in Panel B, with the exception that we drop the districts in Bavaria and Baden Wuerttemberg from the sample and allow for anticipation and treatment effects only 10 days before and 10 days after school reopening.

Figure 9: The Impact of the Summer School Reopenings on Other Age Brackets

A: Raw Data B: Estimates

Age Bracket: 15-34

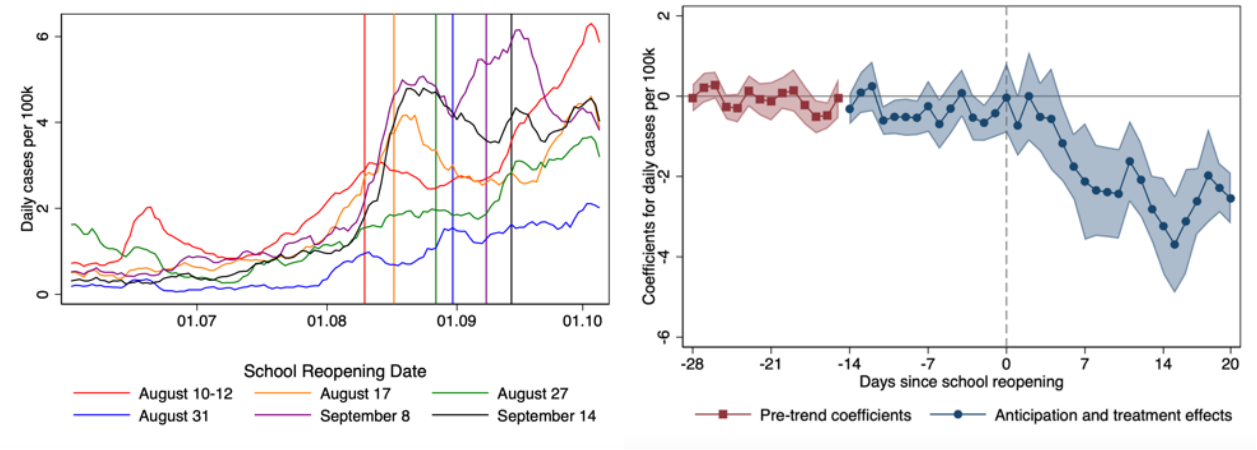

Age Bracket: 35-59

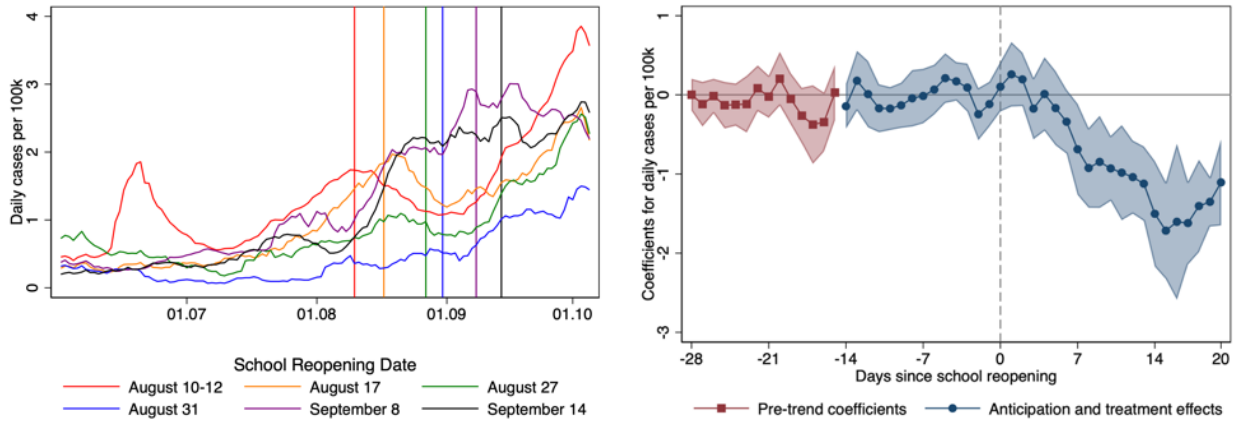

Age Bracket: 60+

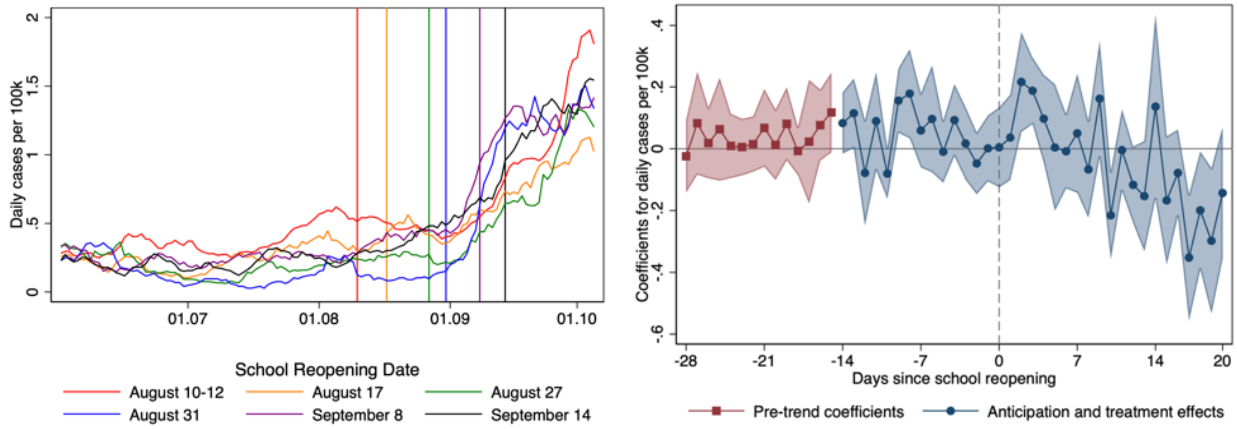

Notes: Panel A displays the daily cases per 100,000 in the respective age bracket, smoothed with a uniformly weighted moving average filter including three lags and three leads. The districts are grouped according to the school reopening date, and the data are shown until October 5 or the day when the fall holiday starts (whichever is earlier). Panel B displays the anticipation and treatment effect estimates using the Borusyak et al. (2020) imputation estimator including district and day fixed effects (blue dots, following equation (2)), as well as OLS estimates for pre-trends (red squares, following equation (3)). Anticipation effects are allowed within 14 days before schools reopen. The outcome variable is defined as the number of daily reported COVID-19 cases (per 100,000 in the respective age bracket) and the districts are weighted according to the age-bracket specific population. The shadows reflect the range inside the 95% coefficient interval, with standard errors clustered at the NUTS-2 level (38 clusters).

Figure 10: The Impact of Summer School Reopenings: Estimates Dropping Southern States

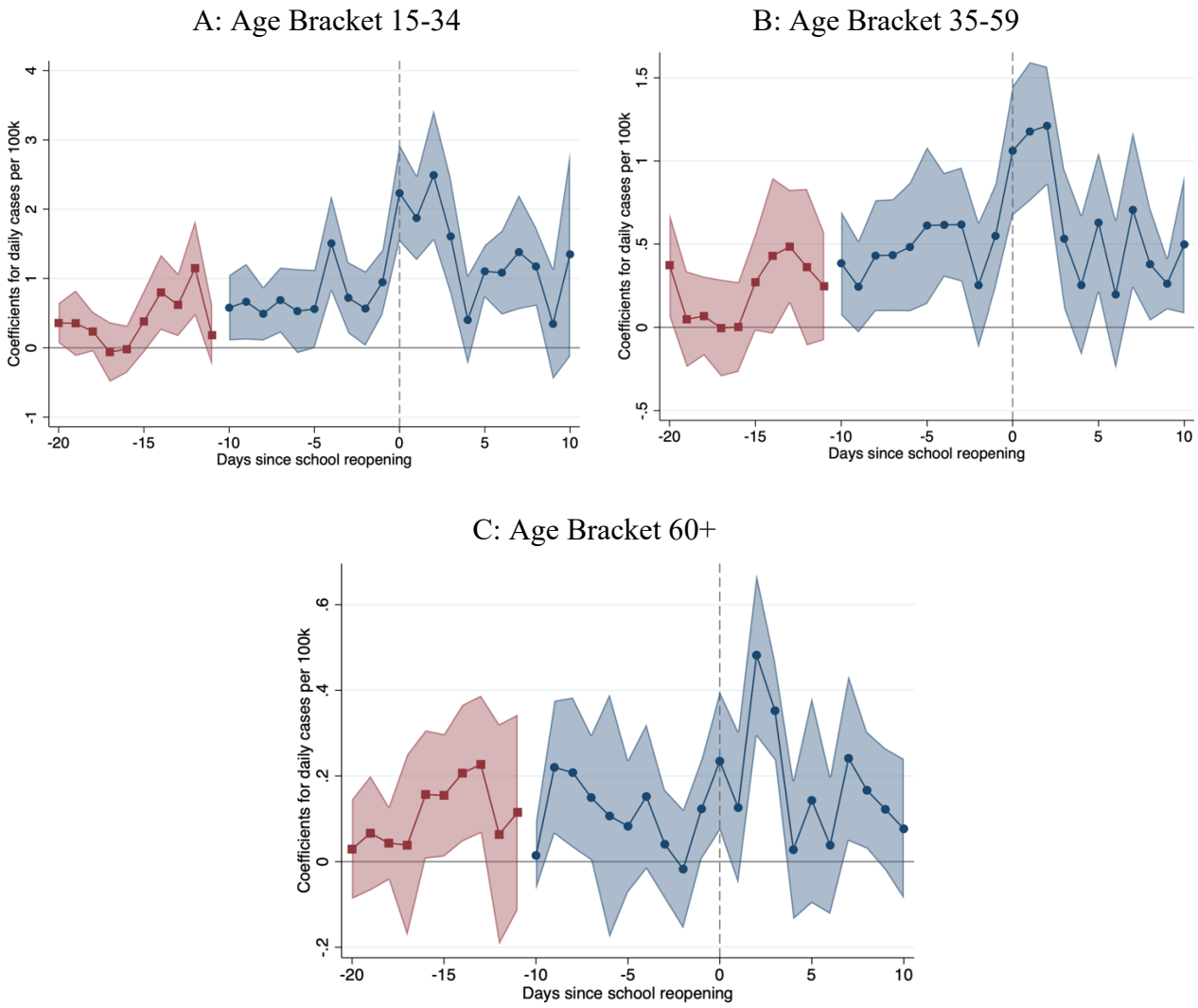

Notes: The three panels, corresponding to different age brackets, display the results from the Borusyak et al. (2020) imputation estimator in specification (2) including district and day fixed effects as well as OLS estimates for pre-trends (red squares, following equation (3)), dropping the districts in Baden Wuerttemberg and Bavaria from the sample. Both anticipation and treatment effects are allowed up to 10 days relative to school reopening. The districts are weighted by the age bracket-specific local population. The shadows reflect the range inside the 95% coefficient interval, with standard errors clustered at the NUTS-2 level (38 clusters).

Figure 11: The Impact of the Summer School Reopenings on Deaths, Age Bracket 60+

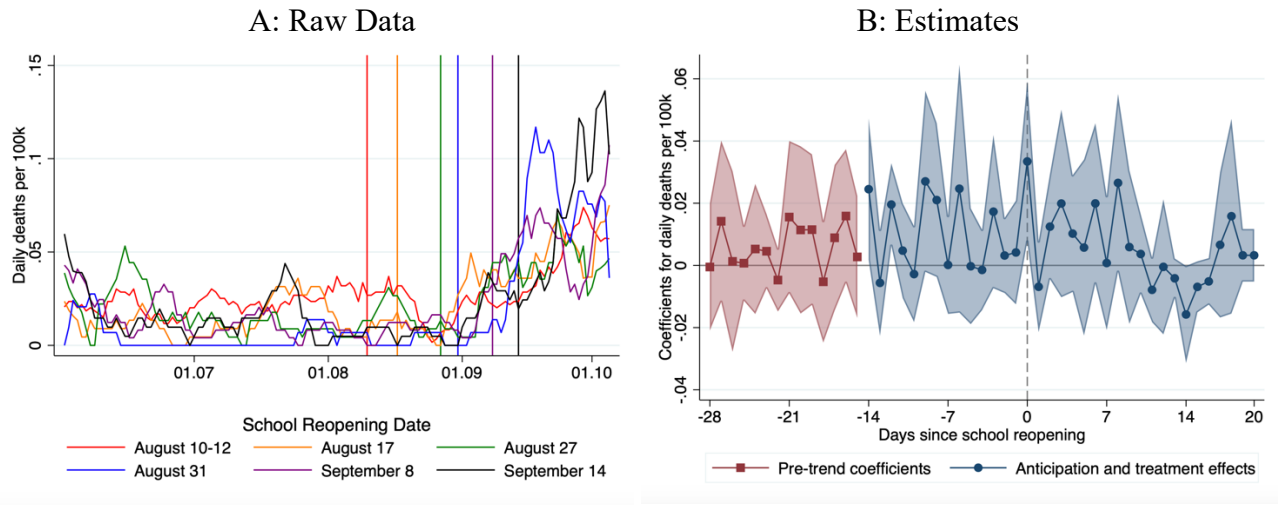

Notes: Panel A displays the daily deaths per 100,000 in the age bracket 60+, smoothed with a uniformly weighted moving average filter including three lags and three leads. The districts are grouped according to the school reopening date, and the data are shown until October 5 or the day when the fall holiday starts (whichever is earlier). Panel B displays the anticipation and treatment effect estimates using the Borusyak et al. (2020) imputation estimator including district and day fixed effects (blue dots, following equation (2)), as well as OLS estimates for pre-trends (red squares, following equation (3)). Anticipation effects are allowed within 14 days before schools reopen. The outcome variable is defined as the number of daily reported COVID-19 deaths (per 100,000 in the age bracket 60+) and the districts are weighted according to the population in the age-bracket 60+. The shadows reflect the range inside the 95% coefficient interval, with standard errors clustered at the NUTS-2 level (38 clusters).

Figure 12: The Impact of the Fall School Closures on Children of Age 5-14

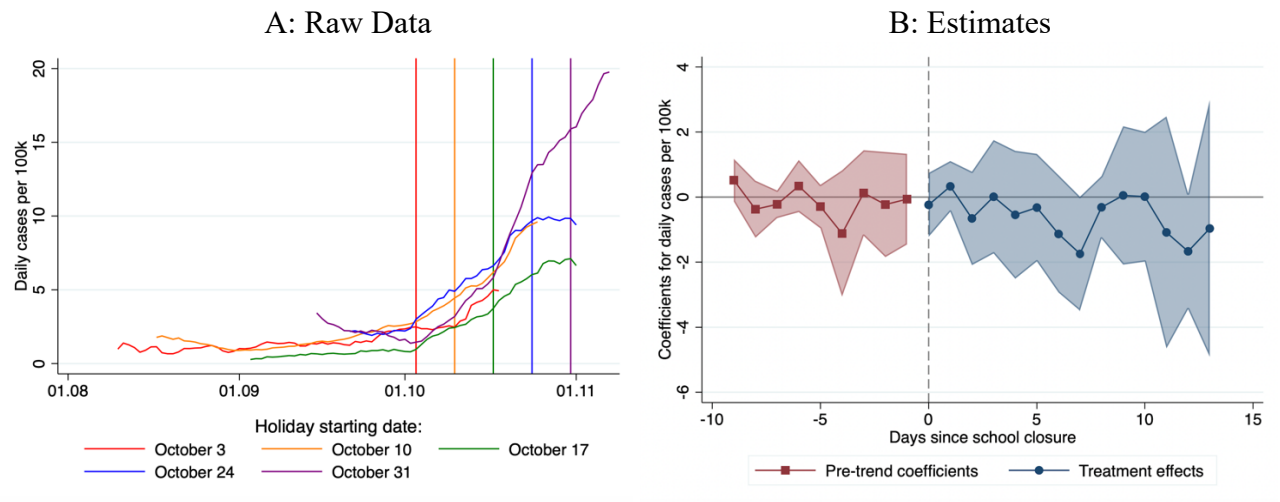

Notes: Panel A displays the daily cases per 100,000 in the age bracket 5-14 years, smoothed with a uniformly weighted moving average filter including three lags and three leads. The districts are grouped according to the holiday starting date, and the data are shown from 7 days after schools reopened after the summer holiday and until the fall holidays end. Panel B displays the treatment effect estimates on the same sample excluding districts in Bavaria, using the Borusyak et al. (2020) imputation estimator including district and day fixed effects (blue squares, following equation (2)), as well as OLS estimates for pre-trends (red squares, following equation (3)). The outcome variable is defined as the number of daily reported COVID-19 cases (per 100,000 in the age bracket 5-14 years), and the districts are weighted according to the population in the age bracket 5-14 years. The shadows reflect the range inside the 95% coefficient interval, with standard errors clustered at the NUTS-2 level (38 clusters).

Figure 13: The Impact of the Fall School Closures on Other Age Brackets

A: Raw Data B: Estimates

Age Bracket: 15-34

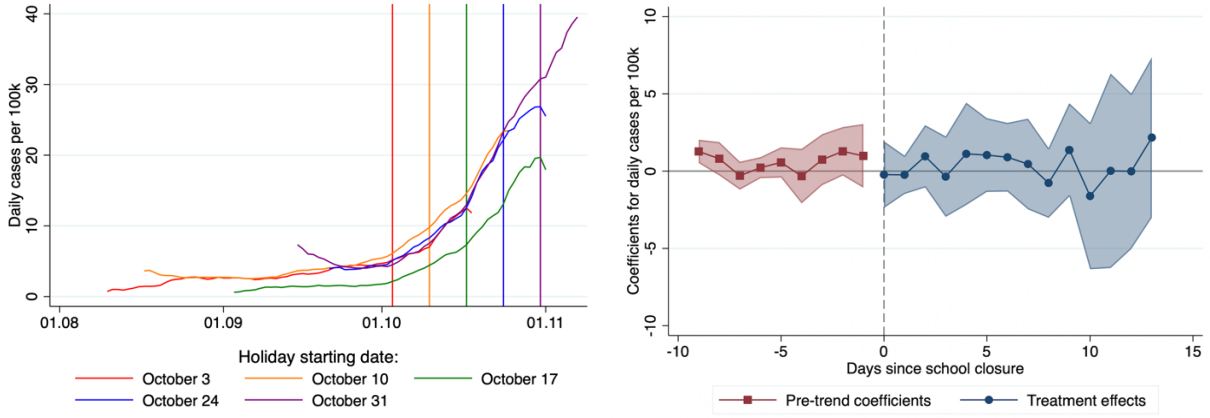

Age Bracket: 35-59

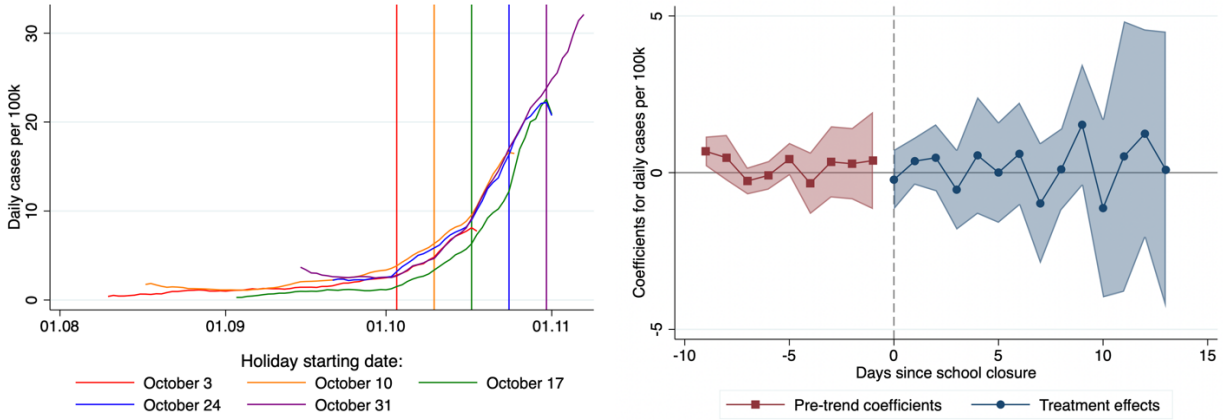

Age Bracket: 60+

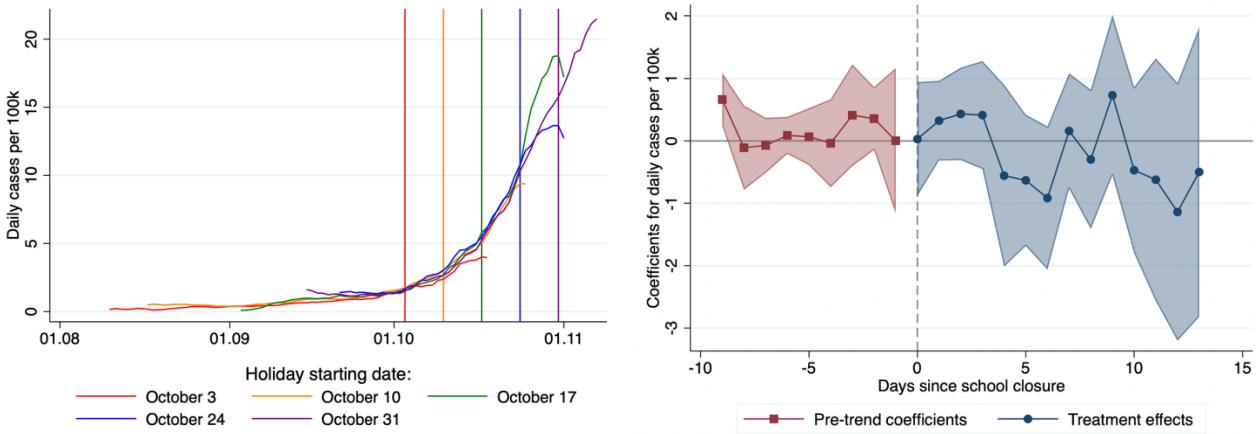

Notes: Panel A displays the daily cases per 100,000 in the respective age bracket, smoothed with a uniformly weighted moving average filter including three lags and three leads. The districts are grouped according to the holiday starting dates, and the data are shown from 7 days after schools reopened after the summer holiday and until the fall holidays end. Panel B displays the anticipation and treatment effect estimates on the same sample excluding districts in Bavaria, using the Borusyak et al. (2020) imputation estimator including district and day fixed effects (blue dots, following equation (2)), as well as OLS estimates for pre-trends (red squares, following equation (3)). The outcome variable is defined as the number of daily reported COVID-19 cases (per 100,000 in the respective age bracket) and the districts are weighted according to the age-bracket specific population. The shadows reflect the range inside the 95% coefficient interval, with standard errors clustered at the NUTS-2 level (38 clusters).

Tables

Table 1: Average Daily Effects of Summer School Closures

Dependent variable	Average daily effects				Mean Incidence Rate
	Week 0	Week 1	Week 2	Weeks 0-2	Week -1
	(1)	(2)	(3)	(4)	(5)
(1) Cases/100k, 5-14 years	-0.140 [-0.361, 0.081]	-0.182 [-0.401, 0.037]	-0.037 [-0.343, 0.269]	-0.120 [-0.329, 0.090]	0.680
(2) Cases/100k, 15-34 years	-0.079 [-0.277, 0.118]	-0.216 [-0.526, 0.094]	-0.297 [-0.772, 0.179]	-0.197 [-0.498, 0.104]	1.069
(3) Cases/100k, 35-59 years	-0.078 [-0.288, 0.133]	-0.278 [-0.557, 0.004]	-0.260 [-0.693, 0.176]	-0.205 [-0.499, 0.091]	0.807
(4) Cases/100k, 60+ years	0.039 [-0.014, 0.092]	0.017 [-0.053, 0.087]	0,053 [-0.049, 0.156]	0.036 [-0.025, 0.097]	0.232
(5) Deaths/100k, 60+ years	0.003 [-0.005, 0.011]	0.009 [0.001, 0.017]	0.016 [0.003, 0.029]	0.009 [0.002, 0.017]	0.010

Notes: This table complements the coefficient plots from Panel B in Figures 5, 6 and 7, providing the average daily coefficients and associated 95% confidence intervals for the imputation estimator. The averages are given for weeks zero (i.e. $h = 0, \ldots, 6$ days since closures; column 1), one and two (columns 2 and 3), and over the first three weeks of summer holiday (column 4) – for all age brackets and for deaths among the population aged 60+. The mean infection rate (per 100,000 inhabitants in the respective age group) in the seven days before schools closed in each state, weighted by the age bracket specific population, is displayed in column 5.

Table 2: Average Daily Effects of School Reopenings

Dependent variable	Anticipation effects		Average daily effects				Mean Incidence Rate
	Week -2	Week -1	Week 0	Week 1	Week 2	Weeks 0-2	Week -1
	(1)	(2)	(3)	(4)	(5)	(6)	(7)
(1) Cases/100k, 5-14 years	0.473 [0.276, 0.670]	0.710 [0.473, 0.946]	1.093 [0.648, 1.538]	-0.905 [-1.317, -0.494]	-1.461 [-2.005, -0.917]	-0.425 [-0.800, -0.049]	2.222
(2) Cases/100k, 15-35 years	-0.307 [-0.576, -0.038]	-0.397 [-0.879, 0.087]	-0.680 [-1.516, 0.156]	-2.260 [-3.188, -1.332]	-2.775 [-3.558, -1.992]	-1.905 [-2.685, -1.131]	2.924
(3) Cases/100k, 35-59 years	-0.068 [-0.293, 0.156]	0.024 [-0.194, 0.241]	-0.014 [-0.318, 0.290]	-0.932 [-1.326, -0.537]	-1.478 [-1.920, -1.035]	-0.808 [-1.150, -0.465]	1.668
(4) Cases/100k, 60+ years	0.067 [0.011, 0.123]	0.029 [-0.033, 0.091]	0.079 [0.016, 0.141]	-0.046 [-0.123, 0.031]	-0.160 [-0.252, -0.068]	-0.043 [-0.107, 0.022]	0.447
(5) Deaths/100k, 60+ years	0.013 [0.002, 0.024]	0.007 [-0.001, 0.015]	0.014 [0.003, 0.024]	0.003 [-0.007, 0.014]	0.000 [-0.011, 0.011]	0.006 [-0.002, 0.014]	0.016

Notes: This table complements the coefficient plots from Panel B in Figures 8, 9, and 11, providing the average daily coefficients and associated 95% confidence intervals for the imputation estimator. The average anticipation effects are displayed in column (1) and (2), for the two weeks prior school start respectively. The averages treatment effects are given for weeks zero (i.e. $h = 0, \ldots, 6$ days since school reopening), one, and two (columns 3-5), and over the first three weeks of summer holiday (column 6) – for all age brackets and for deaths among the population aged 60+. The mean infection rate (per 100,000 inhabitants in the respective age group) in the seven days before schools reopened in each state, weighted by the age-bracket specific population, is displayed in column 7.

Table 3: Average Daily Effects of the Fall Closures

Dependent variable	Average daily effects			Mean Incidence Rate
	Week 0	Week 1	Weeks 0-1	Week -1
	(1)	(2)	(3)	(4)
(1) Cases/100k, 5-14 years	-0.37 [-1.29, 0.56]	-0.82 [-2.41, 0.78]	-0.59 [-1.78, 0.60]	4.08
(2) Cases/100k, 15-34 years	0.45 [-1.24, 2.15]	0.23 [-2.75, 3.21]	0.34 [-1.92, 2.60]	8.72
(3) Cases/100k, 35-59 years	0.18 [-0.77, 1.12]	0.20 [-2.01, 2.40]	0.19 [-1.35, 1.72]	5.67
(4) Cases/100k, 60+ years	-0.13 [-0.59, 0.33]	-0.30 [-1.50, 0.89]	-0.22 [-1.01, 0.58]	3.13

Notes: This table complements the coefficient plots from Panel B in Figures 12 and 13, providing the average daily coefficients and associated 95% confidence intervals for the imputation estimator. The averages are given for weeks zero (i.e. $h = 0, \dots, 6$ days since closures; column 1), one (column 2) and over the first two weeks of summer holiday (column 3) – for all age brackets. The mean infection rate (per 100,000 inhabitants in the respective age group) in the seven days before schools closed in each state, weighted by the age bracket specific population, is displayed in column 4.

Bibliography

Abraham, S.; Sun, L. (2018). Estimating Dynamic Treatment Effects in Event Studies With Heterogeneous Treatment Effects. Working Paper.

Adda, J. (2016). Economic Activity and the Spread of Viral Diseases: Evidence from High Frequency Data. *The Quarterly Journal of Economics*. 131 (2), 891–941.

Alon, T.; Doepke, M.; Olmstead-Rumsey, J.; Tertilt, M. (2020, August). This Time It's different: The Role of Women's Employment in a Pandemic Recession. *IZA Discussion Paper* No. 13562.

Bauer, A.; Weber, E. (2020): COVID-19: How much unemployment was caused by the shutdown in Germany? *Applied Economics Letters.* Database retrieved from: https://iab.de/de/daten/corona-eindaemmungsmassnahmen.aspx.

Bayham, J,; Fenichel, E. (2020, March). The Impact of School Closure for COVID-19 on the US Healthcare Workforce and the Net Mortality Effects. *Cold Spring Harbor Laboratory Press*. 5(5), 271-278.

Berner, R. (2020, July). Immunisierungsgrad geringer als erwartet – Schulen haben sich nicht zu Hotspots entwickelt. *Uniklinikum TU Dresden*. Retrieved from: https://tu-dresden.de/tu-dresden/newsportal/.

Borusyak, K.; Jaravel, X.; Spiess, J. (2020). Revisiting Event Study Designs: Robust and Efficient Estimation. Working Paper.

Chaisemartin, C. de and D'Haultfoeuille, X. (2019). Two-way Fixed Effects Estimators with Heterogeneous Treatment Effects. *American Economic Review*. 110 (9), 2964-2996.

Correia, S.; Guimarães, P.; Zylkin, T. Z. (2020). Fast Poisson estimation with high-dimensional fixed effects. *Stata Journal*. 20(1), 95–115.

Davies, N.; Klepac, P.; Liu, Y.; Prem, K.; Jit, M. (2020, June). Age-dependent effects in the transmission and control of COVID-19 epidemics. *Nature Medicine.* 26(8), 1205-1211.

Deutschlandfunk: Heinemann, C. (2020, August). Wir können uns Reisen in Risikogebiete nicht leisten. Retrieved from: https://www.deutschlandfunk.de.

Engzell, P.; Frey, A.,; Verhagen, M. D. (2020, October). Learning Inequality During the COVID-19 Pandemic. SocArXiv No 31235. Retrieved from: https://doi.org/10.31235/osf.io/ve4z7.

Fateh-Moghadam, P.; Battisti, L.; Molinaro, S.; Dallago, G.; Binkin, N.; Zuccali, M. (2020, July). Contact tracing during Phase I of the COVID-19 pandemic in the Province of Trento, Italy: key findings and recommendations. *Cold Spring Harbor Laboratory.* Working Paper. Retrieved from: https://doi.org/10.1101/2020.07.16.20127357.

Frankfurter Allgemeine Zeitung (2020, June 5). So weit öffnen die Bundesländer ihre Schulen. Retrieved from: https://www.faz.net.

Fontanet, A.; Tondeur, L.; Madec, Y.; Grant, R.; Besombes, C.; Jolly, N.; Fernandes Pellerin, S.; Ungeheuer, M.-N.; Cailleau, I.; Kuhmel, L.; Temmam, S.; Huon, C.; Chen, K.-Y.; Crescenzo, B.; Munier, S.; Demeret, C.; Grzelak, L.; Staropoli, I.; Bruel, T.; Gallian, P.; Cauchemez, S.; van der Werf, S.; Schwartz, O.; Eloit, M.; Hoen, B. (2020, June). Cluster of COVID-19 in northern France: A retrospective closed cohort study. MedRxiv No 1101. Retrieved from: https://doi.org/10.1101/2020.04.18.20071134

Fuchs-Schündeln, N.; Kuhn, M.; Tertilt, M. (2020, June). The Short-Run Macro Implications of School and Child Care Closures. *IZA Discussion Paper*, No. 13353.

Handelsblatt (2020, August 3). Wie die Bundesländer ihre Schulen wieder öffnen. Retrieved from: https://www.handelsblatt.com.

Hanushek, E.; Woessmann, L. (2020, September). The Economic Impacts of Learning Losses. *OECD Education*. Working Paper No 294.

Heald-Sargent, T.; Muller, W.; Zheng, X.; Rippe, J.; Patel, A.; Kociolek, L. (2020, September). Age-Related Differences in Nasopharyngeal Severe Acute Respiratory Syndrome Coronavirus 2 (SARS- CoV-2) Levels in Patients With Mild to Moderate Coronavirus Disease 2019 (COVID-19). *JAMA Pediatrics.* 174(9): 902–903.

Isphording, I.; Lipfert, M.; Pestel, N. (2020, October). School Reopenings after Summer Breaks in Germany Did Not Increase SARS-CoV-2 Cases. *IZA Discussion Paper*, No. 13790.

Jones, T.; Mühlemann, B.; Veith, T.; Biele, G.; Zuchowski, M.; Hoffmann, J.; Stein, A.; Edelmann, A.; Corman, V.; Drosten, C. . (June, 2020). An analysis of SARS-CoV-2 viral load by patient age. MedRxiv No 1101. Retrieved from: https://doi.org/10.1101/2020.06.08.20125484.

New York Times: Leatherby, L.; Jones, L. (2020, August 31). U.S. Coronavirus Rates Are Rising Fast Among Children. Retrieved from: http://www.nytimes.com.

Pouletty, M.; Borocco, C.; Ouldali, N., Caseris, M.; Basmaci, R.; Lachaume, N.; Bensaid, P.; Pichard, S.; Kouider, H.; Morelle, G.; Craiu, I.; Pondarre, C.; Deho, A.; Maroni, A.; Oualha, M.; Amoura, Z.; Haroche, J.; Chommeloux, J.; Bajolle, F.; Beyler, C.; Bonacorsi, S.; Carcelain, G.; Koné-Paut, I.; Bader-Meunier, B.; Faye, A.; Meinzer, U.; Galeotti, C.; Melki, I. (2020, June). Paediatric multisystem inflammatory syndrome temporally associated with SARS-CoV-2 mimicking Kawasaki disease (Kawa-COVID-19): a multicentre cohort. Annals of the Rheumatic Diseases. 79(8), 999–1006.

Santos Silva, J., Tenreyro, S. (2006). The log of gravity. The Review of Economics and statistics. 88(4), 641-658.

Süddeutsche Zeitung (2020, March 21). Diese Einschränkungen gelten in den Bundesländern. Retrieved from: https://www.sueddeutsche.de.

The Guardian: McIntyre, N.; Duncan, P. (2020, September 7). Coronavirus cases rise steeply among young people in England. Retrieved from: https://www.theguardian.com.

The Telegraph: Turner, C. (2020, October 16). Teachers call for “circuit-breaker” lockdown and

two-week half term. Retrieved from: https://www.telegraph.co.uk.

Viner, R.; Russell, S.; Croker, H.; Packer, J.; Ward, J.; Stansfield, C.; Mytton, O.; Bonell, C.; Booy, R. (2020, May). “School closure and management practices during coronavirus outbreaks including COVID-19: a rapid systematic review”. *The Lancet Child & Adolescent Health*. 4(5), 397-404.

Wang, Z.; Zhou, Q.; Wang, C.; Shi, Q.; Lu, S.; Ma, Y.; Luo, X.; Xun, Y.; Li, W.; Baskota, M.; Yang, Y.; Zhai, H.; Fukuoka, T.; Ahn, H.; Lee, M.; Luo, X.; Liu, E., Chen, Y. (2020, May). Clinical characteristics of children with COVID-19: a rapid review and meta-analysis. Annals of translational medicine. 8(10), 620.

ZEIT: Erdmann, E. (2020, September 18). Die Ruhe könnte trügerisch sein. Besonders junge Menschen stecken sich an. Retrieved from: https://www.zeit.de.

Appendix: Additional Figures

Figure A1: Summer School Closures – OLS Estimates from a Conventional Event Study

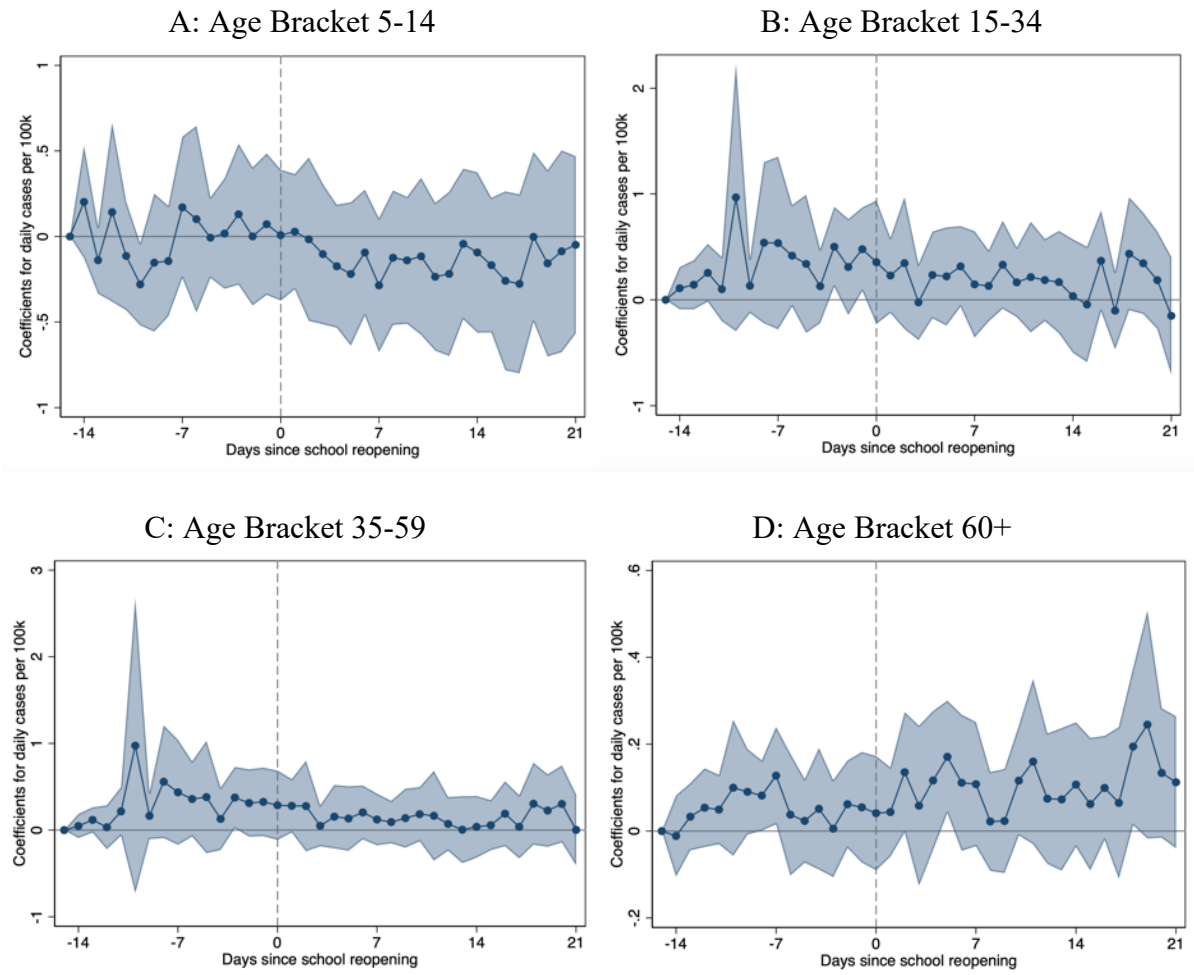

Notes: The four panels, corresponding to different age brackets, display the estimates from the conventional event study specification (4) estimated by OLS with district and day fixed effects. We assume zero effects 15 or more days prior to the school closure event and drop the observations 21 and more days after the event. The regressions are weighted by the age bracket-specific local population. The shadows reflect the range inside the 95% coefficient interval, with standard errors clustered at the NUTS-2 level (38 clusters).

Figure A2: Summer School Closures - Estimates from a Poisson Pseudo-Maximum Likelihood Regression

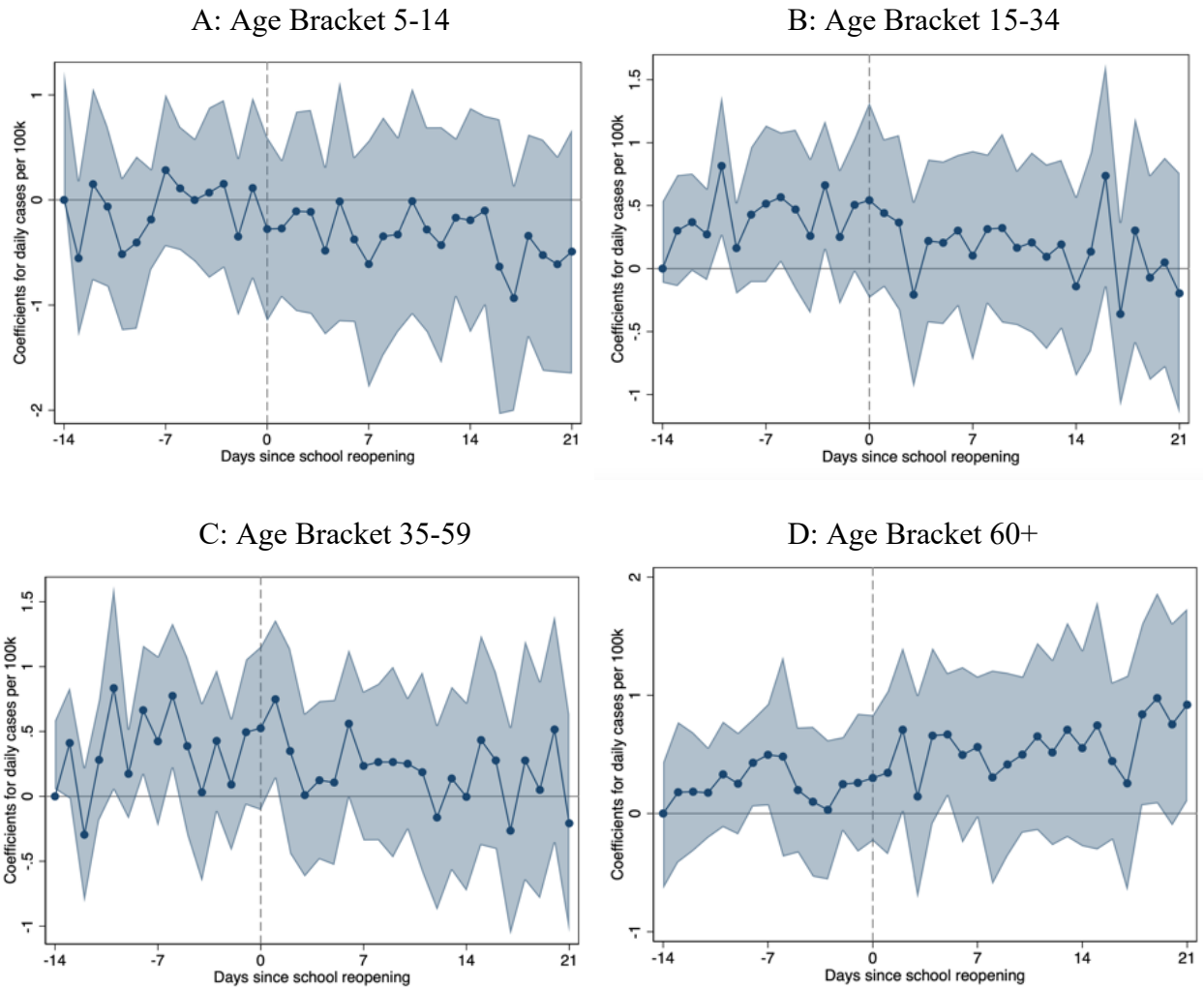

Notes: The four panels, corresponding to different age brackets, display the estimates from the Poisson pseudo-maximum likelihood specification described by (5), with district and day fixed effects. We assume zero effects 15 or more days prior to the school closure event and drop the observations 21 and more days after the event. The regressions are weighted by the age bracket-specific local population. The shadows reflect the range inside the 95% coefficient interval, with standard errors clustered at the NUTS-2 level (38 clusters).

Figure A3: School Reopening after Summer Holidays – OLS Estimates from a Conventional Event Study

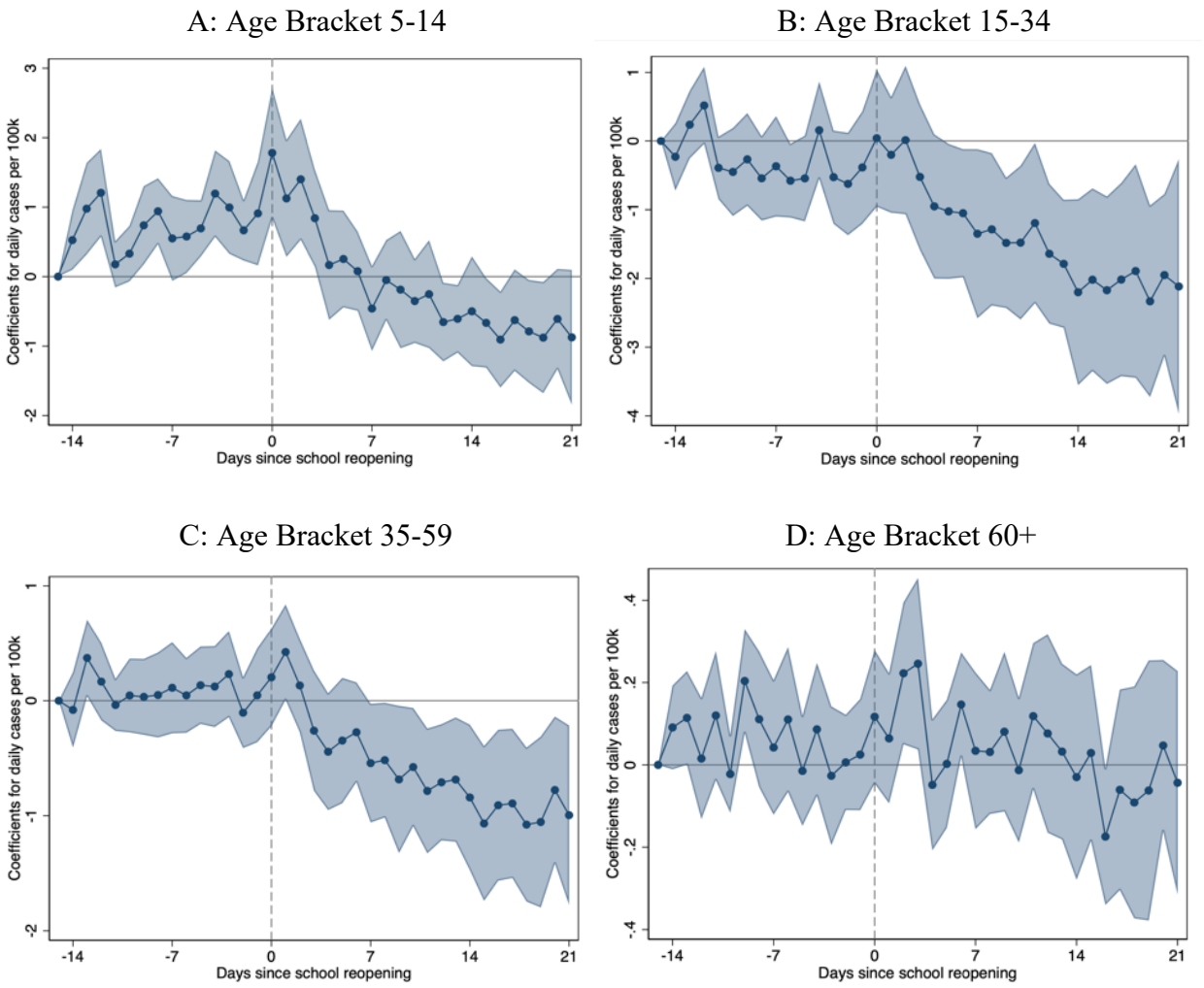

Notes: The four panels, corresponding to different age brackets, display the estimates from the conventional event study specification (4) estimated by OLS with district and day fixed effects. We assume zero effects 15 or more days prior to the school reopening event and drop the observations 21 and more days after the event. The regressions are weighted by the age bracket-specific local population. The shadows reflect the range inside the 95% coefficient interval, with standard errors clustered at the NUTS-2 level (38 clusters).

Figure A4: School Reopening after Summer Holidays- Estimates from a Poisson Pseudo-Maximum Likelihood Regression

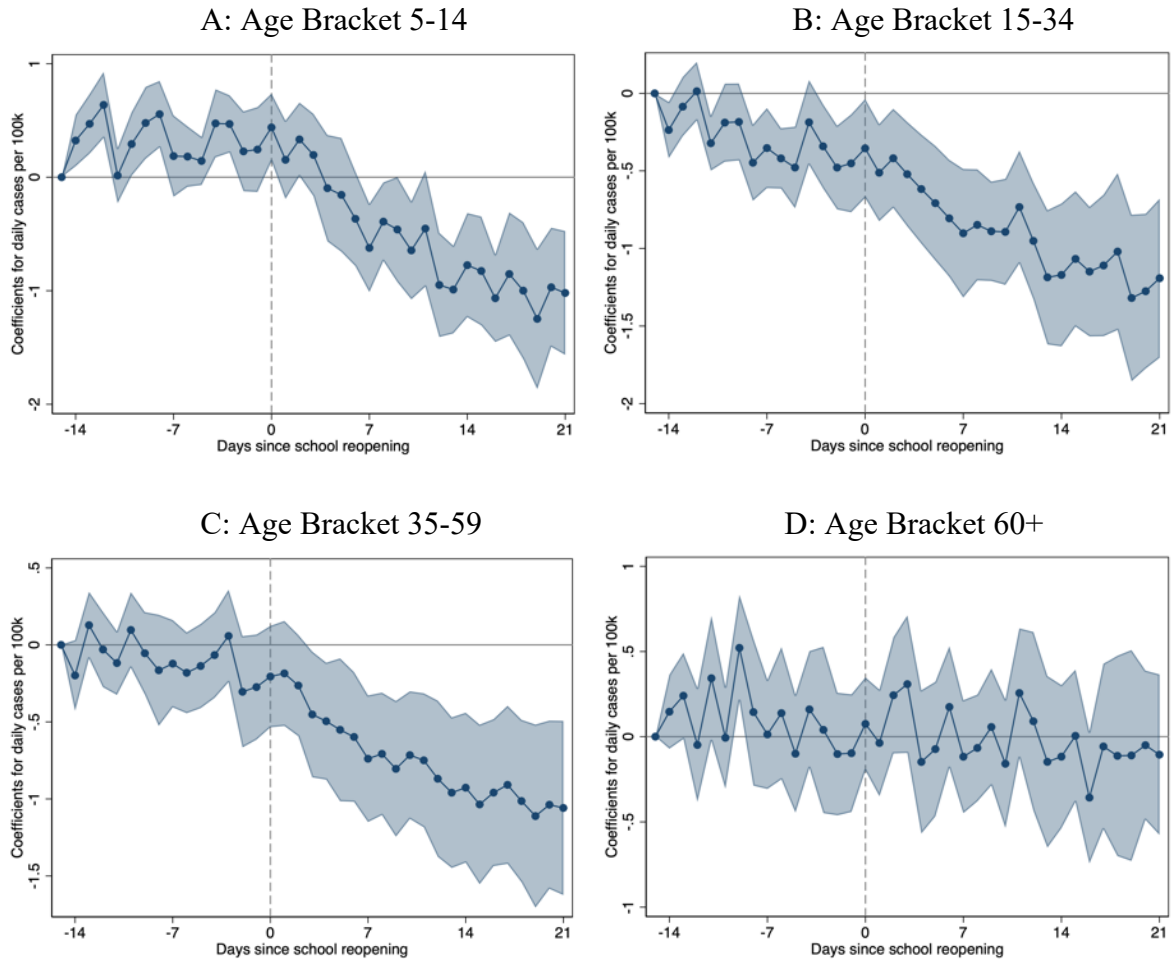

Notes: The four panels, corresponding to different age brackets, display the estimates from the Poisson pseudo-maximum likelihood specification described by (5), with district and day fixed effects. We assume zero effects 15 or more days prior to the school reopening event and drop the observations 21 and more days after the event. The regressions are weighted by the age bracket-specific local population. The shadows reflect the range inside the 95% coefficient interval, with standard errors clustered at the NUTS-2 level (38 clusters).

Figure A5: Fall School Closures – OLS Estimates from a Conventional Event Study

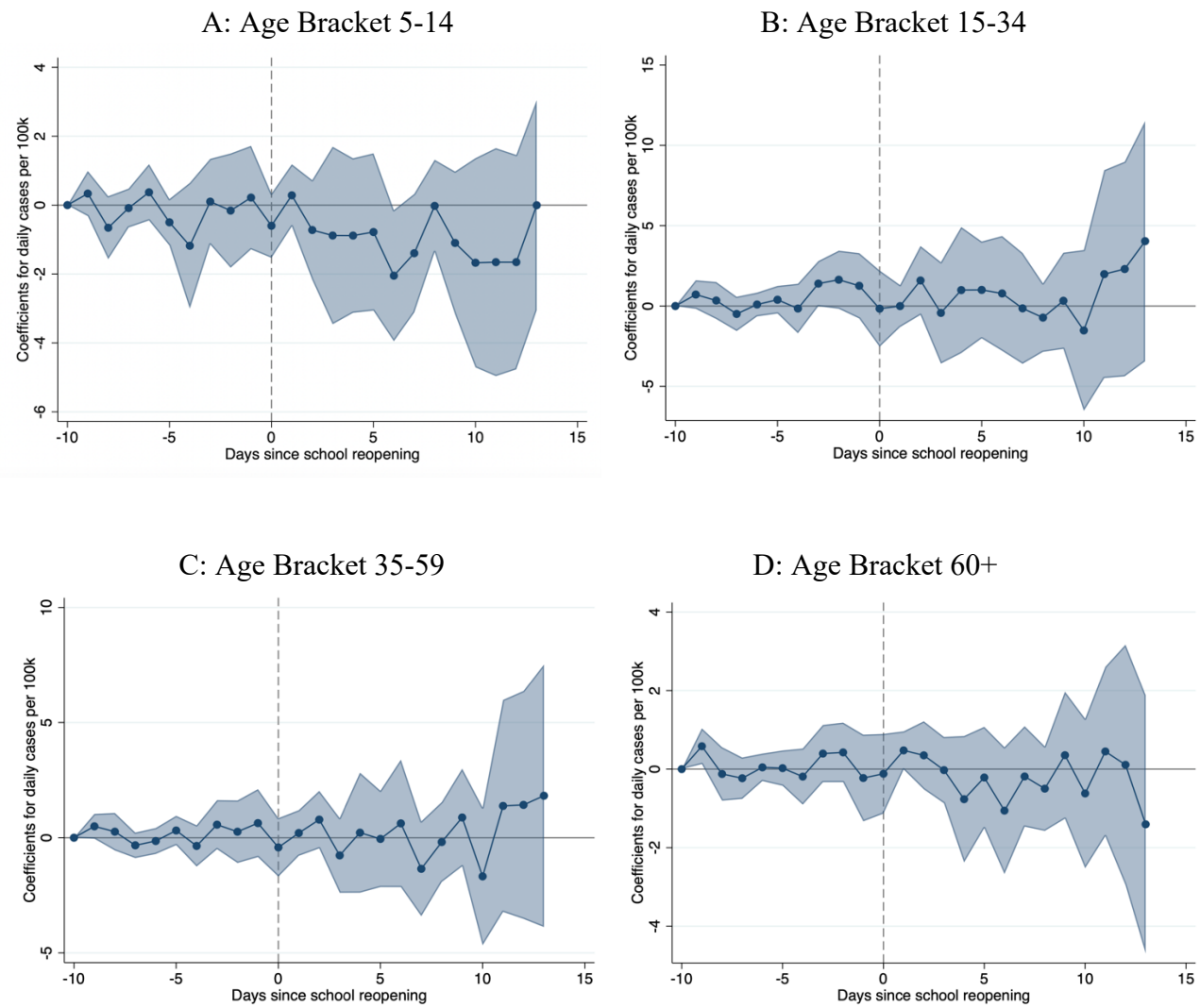

Notes: The four panels, corresponding to different age brackets, display the estimates from the conventional event study specification (4) estimated by OLS with district and day fixed effects. The sample includes observations from 7 days after schools reopen after the summer holiday until the fall holiday end; we exclude all districts in Bavaria. We assume zero effects 10 or more days prior to the fall school closure event and drop the observations 14 and more days after the event. The regressions are weighted by the age bracket-specific local population. The shadows reflect the range inside the 95% coefficient interval, with standard errors clustered at the NUTS-2 level (38 clusters).

Figure A6: Fall School Closures - Estimates from a Poisson Pseudo-Maximum Likelihood Regression

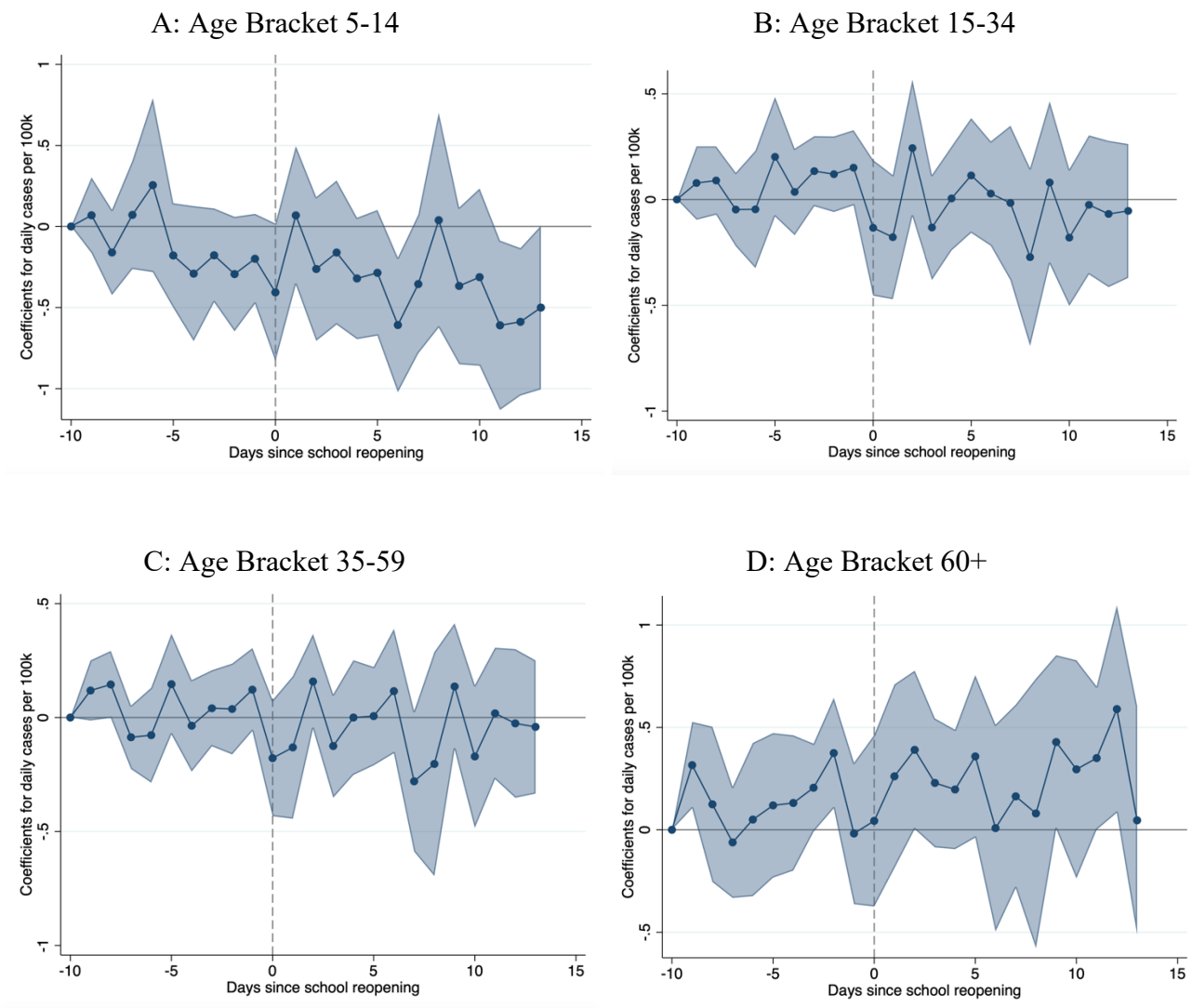

Notes: The four panels, corresponding to different age brackets, display the estimates from the Poisson pseudo-maximum likelihood specification described by (5), with district and day fixed effects. The sample includes observations from 7 days after schools reopen after the fall holiday until the fall holiday end; we exclude all districts in Bavaria. We assume zero effects 10 or more days prior to the school closure event and drop the observations 14 and more days after the event. The regressions are weighted by the age bracket-specific local population. The shadows reflect the range inside the 95% coefficient interval, with standard errors clustered at the NUTS-2 level (38 clusters).